Mixed Dimer Configuration Model in Type D Cluster Algebras

Gregg Musiker*

Department of Mathematics University of Minnesota Minnesota, U.S.A.

musiker@umn.edu

Kayla Wright

Department of Mathematics University of Minnesota Minnesota, U.S.A.

kaylaw@umn.edu

Submitted: May 17, 2021; Accepted: Jan 24, 2023; Published: May 5, 2023 © The authors. Released under the CC BY-ND license (International 4.0).

Abstract

We define a combinatorial model for F-polynomials and g-vectors for type D_n cluster algebras where the associated quiver is acyclic. Our model utilizes a combination of dimer configurations and double dimer configurations which we refer to as mixed dimer configurations. In particular, we give a graph theoretic recipe that describes which monomials appear in such F-polynomials, as well as a graph theoretic way to determine the coefficients of each of these monomials. In addition, we prove that a weighting on our mixed dimer configuration model yields the associated g-vector. To prove this formula, we use a combinatorial formula due to Thao Tran (arXiv:0911.4462, 2009) and provide explicit bijections between her combinatorial model and our own.

Mathematics Subject Classifications: 13F60, 82B20, 06A07

1 Introduction

Positivity of the coefficients in the Laurent expansions of cluster variables was a longrunning open question in the theory of cluster algebras, until it was proven around 2014 [LS15, GHKK18]. Even with positivity verified, explicit combinatorial interpretations for the Laurent expansions as generating functions has still been a question of active research for many different cluster algebras. In the case of cluster algebras of classical type, i.e. those defined by a (valued) quiver mutation-equivalent to a Dynkin Diagram of type A_n , B_n , C_n , or D_n , there are various such interpretations in the literature. For example, see [Mus07, FZ03b, Tra09, YZ08] depending on whether the initial quiver is bipartite, acyclic,

^{*}Supported by NSF grant DMS-1745638 and DMS-1854162.

or more general. The Caldero-Chapoton formula, as first appearing in [CC06] for ADE types, also yields positive formulas, modulo verification that the Euler characteristics of the relevant quiver Grassmannians are positive.

Furthermore, when a cluster algebra comes from a surface, there is a combinatorial interpretation of cluster variables via the language of snake graphs [MSW11]. The only cluster algebras that are both of classical type and from a surface are those of type A_n or type D_n . Such cluster algebras are associated to triangulations of (n + 3)-gons or once-punctured n-gons, respectively.

Going beyond cluster algebras of classical type or cluster algebras from surfaces, there are families of cluster algebras associated to coordinate rings of the Grassmannians [Sco06], or more generally positroid varieties [Pos06, GL19]. For such cluster algebras, a finite subset of cluster variables (namely those parametrized by Plücker coordinates), admit combinatorial interpretations using (almost) perfect matchings of plabic graphs. Such interpretations are often packaged together into what Postnikov called the boundary measurement map. See [Lam15, MS16, MS17]. However, beginning with examples such as cluster algebras associated to the Grassmannian of 3-planes in 6-space, additional cluster variables lack such an interpretation.

Another rich source of cluster algebras, which contain (toric) cluster variables with combinatorial interpretations also given via dimers on bipartite graphs, are those associated to the octahedron recurrence [Spe07], Gale-Robinson sequences [Spe07, BMPW09], T-systems [DF14], or brane tilings [EF12, FHV $^+$ 06, HV07]. The first author has in particular studied such cases in [JMZ13, LMNT14, LM17, LM20]. We also note the work of [Gli11] which focused on related cluster algebras, but explicitly focused on Y-system and F-polynomial interpretations rather than expansions of cluster variables.

More recent work [KP16], also see [LM20], has developed (and proven or conjectured) a double dimer configuration combinatorial interpretation for cluster variables whose Laurent expansions were previously not understood combinatorially. Related work appears in [Lam15, Sections 3-4], where products of exactly two (resp. three) Plücker coordinates are interpreted as Temperley-Lieb Immanants (resp. webs). See also the work of [Jen19] that shows that partition functions of double dimers on certain graphs with nodes satisfy three-term identities. With these examples in mind, we have returned to the classical case of type D_n cluster algebras arising from acyclic quivers with an eye towards a combinatorial interpretation for Laurent expansions of cluster variables that utilized a mixture of dimer configurations and double dimer configurations. To this end, we demonstrate a combinatorial interpretation via mixed dimer configurations for F-polynomials in the case of acyclic quivers of type D_n . Thanks to the separation of addition formulae of Fomin and Zelevinsky [FZ07], the F-polynomials and g-vectors provide as much information as the Laurent expansions of the cluster variables (with principal coefficients) themselves. We anticipate that this new interpretation will provide further insight into the conjectured mixed dimer configuration combinatorial interpretations arising in [LM20], or allow the generalization of techniques using weighted decompositions of Quiver Grassmannian as in [GW17].

We begin this paper by reviewing the basics of cluster algebras in Section 2. We then describe our combinatorial model, culminating with our main theorem for F-polynomials in Section 3. The proof of this theorem (Theorem 35) is given in Section 4 by introducing Thao Tran's model from [Tra09] and then showing the two directions of our combinatorial bijection. In Section 5, we complete the picture by providing an approach for reading off the associated g-vector from the minimal matching M_{-} associated to Q and \underline{d} as part of our model. This allows for the computation of the Laurent expansion for the associated cluster variables as well. We end with a discussion of future directions in Section 6.

Acknowledgements: The authors would like to thank the support of the NSF, grants DMS-1745638 and DMS-1854162. We would also like to thank Esther Banaian, Sebastian Franco, Helen Jenne, Rick Kenyon, David Speyer, and Lauren Williams for many helpful conversations. We additionally thank the anonymous referee whose suggestions improved our exposition. Lastly, we would like to acknowledge the REU report from University of Minnesota's 2018 Summer REU for inspiration and insightful examples [PW18].

2 Background

2.1 Cluster Algebra Basics

Cluster algebras were originally defined by Fomin and Zelevinsky in [FZ02] in order to give a combinatorial characterization of total positivity and canonical bases in algebraic groups, but have since been found to be helpful in many other areas of mathematics such as algebraic combinatorics, symplectic geometry, Teichmüller theory, and even some areas of physics. Loosely speaking, a cluster algebra is a certain commutative algebra generated by a distinguished set of generators called cluster variables. To obtain these cluster variables, we start with an initial seed, which consists of n cluster variables as well as a quiver or an exchange matrix. Using the quiver/exchange matrix, we mutate in the k^{th} direction, transforming our original set of cluster variables into a new set where we change the k^{th} cluster variable for a new expression in the rest of the variables based on the binomial exchange relation. After mutation, we obtain a new seed containing a new set of cluster variables and we iterate mutation in all possible directions. The total set of resulting cluster variables generates the cluster algebra.

In [FZ07], the notion of F-polynomials and g-vectors were introduced which gave a formula for cluster variables in terms of data only dependent on the initial seed. So, once the F-polynomial and associated g-vectors are computed, we can recover the Laurent polynomial expansion for the associated cluster variable.

2.1.1 Defining a Cluster Algebra

In this section, we formally define a cluster algebra of geometric type following [FWZ16].

Definition 1. Let J be a finite set and let $\text{Trop}(u_j : j \in J)$ be an abelian group with respect to multiplication freely generated by the elements u_j for $j \in J$. Define **tropical plus**, denoted \oplus , via

$$\prod_{j} u_j^{a_j} \oplus \prod_{j} u_j^{b_j} := \prod_{j} u_j^{\min(a_j, b_j)}.$$

Call Trop $(u_j: j \in J)$ a **tropical semifield** with respect to multiplication and \oplus .

Remark 2. If $J = \emptyset$, then we obtain the trivial semifield consisting of the single element 1. The group ring of $\text{Trop}(u_j : j \in J)$ is the ring of Laurent polynomials in the variables u_j .

Let $m, n \in \mathbb{Z}_{>0}$ such that $m \ge n$ and let $\mathbb{P} = \text{Trop}(x_{n+1}, \dots, x_m)$. Let \mathcal{F} be the field of fractions in n algebraically independent variables with coefficients in \mathbb{QP} , the field of fractions of the group ring \mathbb{ZP} .

Definition 3. A labeled seed in \mathcal{F} is a pair (\tilde{x}, \tilde{B}) where

- $\tilde{x} = (x_1, \dots, x_n, x_{n+1}, \dots, x_m)$ is the **extended cluster** where x_1, \dots, x_n are algebraically independent over \mathbb{QP} and $\mathcal{F} = \mathbb{QP}(x_1, \dots, x_n)$ and
- \tilde{B} is the **extended exchange matrix** i.e. an $m \times n$ matrix over \mathbb{Z} such that the top $n \times n$ submatrix B is skew-symmetrizable. That is, the top $n \times n$ submatrix B can be written as a skew symmetric matrix of the form DB for some $n \times n$ diagonal matrix D with positive integer diagonal entries. B is called the **principal part** of the exchange matrix.

Remark 4. If we restrict our attention to a skew-symmetric cluster algebra of geometric type, we can replace the notion of an exchange matrix with a quiver.

Definition 5. Let $1 \leq k \leq n$. An $m \times n$ matrix \tilde{B}' is obtained by **matrix mutation in** the k^{th} direction from \tilde{B} if the entries of $\tilde{B}' = (b'_{ij})$ are given by

$$b'_{ij} = \begin{cases} -b_{ij} & \text{if } i = k \text{ or } j = k \\ b_{ij} + \operatorname{sgn}(b_{ik}) \max(b_{ik}b_{kj}, 0) & \text{otherwise} \end{cases}$$

Definition 6. Let $(\tilde{x}, \tilde{B} = (b_{ij}))$ be a labeled seed in \mathcal{F} . Seed mutation μ_k in the k^{th} direction transforms (\tilde{x}, \tilde{B}) into the labeled seed $\mu_k(\tilde{x}, \tilde{B}) = (\tilde{x}', \tilde{B}')$ where

• $\tilde{x}' = (x_1, \dots, x_k', \dots, x_n)$ where

$$x'_{k} = x_{k}^{-1} \left(\prod_{i=1}^{m} x_{i}^{\max(b_{ik},0)} + \prod_{i=1}^{m} x_{i}^{\max(-b_{ik},0)} \right)$$

• \tilde{B}' is obtained by matrix mutation in the direction k.

Remark 7. In the skew-symmetric case, there is a notion of quiver mutation that is completely graph theoretic.

Definition 8. Let \mathbb{T}_n be the *n*-regular tree. A **cluster pattern** is an assignment of labeled seed $(\tilde{x}_t, \tilde{B}_t)$ to every vertex $t \in \mathbb{T}_n$ such that if $t \xrightarrow{k} t'$, then the seeds labeled by t and t' are obtained from one another via mutation in the k^{th} direction. Write $\tilde{x}_t = (x_{1;t}, \ldots, x_{m;t})$ and $\tilde{B}_t = (b_{ij}^t)$.

Definition 9. Given a cluster pattern $\{(\tilde{x}_t, \tilde{B}_t)\}_{t \in \mathbb{T}_n}$, we let \mathcal{X} denote the set of all cluster variables, i.e.

$$\mathcal{X} := \{ x_{j;t} : 1 \leqslant j \leqslant n, t \in \mathbb{T}_n \}.$$

The **cluster algebra** associated to a given cluster pattern is the \mathbb{ZP} subalgebra of \mathcal{F} generated by all of the cluster variables, i.e. we set $\mathcal{A} = \mathbb{ZP}[\mathcal{X}]$.

One of the first fundamental properties proven about cluster algebras is the **Laurent Phenomenon**.

Theorem 10. [FZ02, Theorem 3.1] For $j \in [n]$ and $t \in \mathbb{T}_n$, any cluster variable $x_{j;t} \in \mathcal{A}$ can be expressed as

$$x_{j;t} = \frac{N(x_1, \dots, x_n)}{x_1^{d_1} \cdots x_n^{d_n}}$$

where $N(x_1, ..., x_n) \in \mathbb{Z}[x_{n+1}^{\pm 1}, ..., x_m^{\pm 1}][x_1, ..., x_n]$ and is not divisible by any x_i . The **denominator vector** of $x_{j;t}$ is the vector $\underline{d} = (d_1, ..., d_n)$ and the denominator vector \underline{d} only depends on B^0 , the principal part of the exchange matrix, rather than on \tilde{B}^0 , the extended exchange matrix.

It took another decade-and-a-half, but a related fundamental theorem is **Laurent Positivity**.

Theorem 11. [LS15, Theorem 1.1]/[GHKK18, Theorem 4.10] Under the same hypotheses as Theorem 10, the polynomial $N(x_1, \ldots, x_n)$, appearing in the numerator for the Laurent expansion of $x_{j;t}$, is not only in $\mathbb{Z}[x_{n+1}^{\pm 1}, \ldots, x_m^{\pm 1}][x_1, \ldots, x_n]$, but is in fact in $\mathbb{Z}_{\geq 0}[x_{n+1}^{\pm 1}, \ldots, x_m^{\pm 1}][x_1, \ldots, x_n]$.

2.1.2 F-Polynomials and g-Vectors

Fix an $n \times n$ skew-symmetrizable matrix $B^0 = (b_{ij}^0)$ over \mathbb{Z} and an initial vertex $t_0 \in \mathbb{T}_n$. Note that a choice of an initial labeled seed $(\tilde{x}_{t_0}, \tilde{B}^0)$ determines a cluster pattern. Here, \tilde{B}^0 is an extended exchange matrix which has B^0 as its principal part, and \tilde{x}_{t_0} is an extended cluster of the appropriate size.

Definition 12. A cluster algebra \mathcal{A} has **principal coefficients at** t_0 if $\tilde{x}_{t_0} = (x_1, \dots, x_{2n})$ and the exchange matrix at t_0 is the **principal matrix** corresponding to B^0 given by

$$\tilde{B}^{t_0} = \begin{pmatrix} B^0 \\ I \end{pmatrix}$$

where I is the $n \times n$ identity matrix. Denote this cluster algebra by $\mathcal{A}_{\bullet} = \mathcal{A}_{\bullet}(B^0, t_0)$. Using the initial cluster of \mathcal{A}_{\bullet} , define the new variables for $1 \leq j \leq n$

$$\hat{y}_j = x_{n+j} \prod_{i=1}^n x_i^{b_{ij}^0}.$$

Using these new variables, we are ready to define the F-polynomial and g-vectors.

Definition 13. Let $1 \leq \ell \leq n$, $t \in \mathbb{T}_n$. There exists a unique primitive polynomial

$$F_{\ell;t} = F_{\ell;t}^{B^0;t_0} \in \mathbb{Z}[u_1, \dots, u_n]$$

and a unique vector $g_{\ell;t} = g_{\ell;t}^{B^0;t_0} = (g_1,\ldots,g_n) \in \mathbb{Z}^n$ such that the cluster variable $x_{\ell;t} \in \mathcal{A}_{\bullet}(B^0,t_0)$ is given by

$$x_{\ell;t} = F_{\ell;t}^{B^0;t_0}(\hat{y_1},\dots,\hat{y_n})x_1^{g_1}\cdots x_n^{g_n}.$$

The polynomial $F_{\ell;t}$ is called an **F-polynomial** and $g_{\ell;t}$ is called a **g-vector**.

The importance of F-polynomials and g-vectors is motivated by the following fundamental "separation of additions" property of cluster algebras of geometric type.

Theorem 14. [FZ07, Theorem 3.7/Corollary 6.3] Given a cluster algebra \mathcal{A} defined over an arbitrary semifield \mathbb{P} with an initial labeled seed $(\tilde{x}_{t_0}, \tilde{B}^0)$, then all cluster variables in \mathcal{A} can be expressed as

$$x_{i,t} = \frac{F_{i,t}^{B^0;t_0}(\hat{y}_1,\dots,\hat{y}_n)x_1^{g_1}\dots x_n^{g_n}}{F_{i,t}^{B^0,t_0}|_{\mathbb{P}}(y_1,\dots y_n)}.$$

In the denominator, the expression is evaluated in \mathbb{P} using ordinary multiplication and \oplus .

In particular, computing the patterns of F-polynomials $\{F_{i;t}\}_{i\in[n];\ t\in\mathbb{T}_n}$ and g-vectors $\{g_{i;t}\}_{i\in[n];\ t\in\mathbb{T}_n}$ is sufficient for deriving the cluster pattern $\{\tilde{x}_t\}_{t\in\mathbb{T}_n}$ regardless of the choice of initial coefficients, i.e. the choice of initial extended exchange matrix \tilde{B}^0 .

Because of Theorems 11 and 14, the F-polynomials arising from a cluster algebra have positive integer coefficients. This observation motivates our desire to have a direct combinatorial explanation for this positivity and integrality, which motivates the combinatorial interpretation studied in this paper.

2.2 Cluster Algebras and Finite Type Classification

In our combinatorial model, we define a graph theoretic interpretation of the F-polynomial in "type D." In particular, one of the most striking results about cluster algebras is that the classification of *finite type* cluster algebras is parallel to that of the Cartan-Killing classification of complex simple Lie algebras, or equivalently of crystallographic finite root systems. Such Lie algebras are modeled by finite type Dynkin diagrams, which are built out of irreducible diagrams coming from four infinite families or from five exceptional cases: $A_n, B_n, C_n, D_n, E_6, E_7, E_8, F_4, G_2$.

Definition 15. We say that a cluster algebra is of **finite type** it is has finitely many seeds.

Definition 16. Let B be an $n \times n$ exchange matrix. The **diagram of** B, denoted $\Gamma(B)$, is the weighted directed graph on nodes v_1, \ldots, v_n with v_i directed towards v_j if and only if $b_{ij} > 0$ and weighted by $|b_{ij}b_{ji}|$.

Theorem 17. [FZ03a] The cluster algebra A is of finite type if and only if it has a seed (x, B) such that $\Gamma(B)$ is an orientation of a finite type Dynkin diagram.

If the conditions of the above theorem hold, \mathcal{A} is of finite type X where X is one of $A_n, B_n, C_n, D_n, E_6, E_7, E_8, F_4, G_2$, as determined by the Dynkin diagram.

2.2.1 F-polynomials and Positive Roots

In order to show the connection of F-polynomials to types of a cluster algebra, we have the following setup. Suppose that B^0 is an acyclic $n \times n$ exchange matrix of type A_n, B_n, C_n , or D_n i.e. $b_{ij} = \pm a_{ij}$ where (a_{ij}) is the Cartan matrix of the corresponding type. Let $\mathcal{A}(B^0, t_0)$ be any cluster algebra which has the extended cluster $(x_1, \ldots, x_n, x_{n+1}, \ldots, x_m)$. By the Laurent phenomenon, Theorem 10, we can associate a denominator vector \underline{d} to each cluster variable $x_{i;t}$ in a given cluster algebra. For acyclic finite type cluster algebras, such denominator vectors can be described concisely as follows.

Theorem 18. [FZ03a, Theorem 1.9] Suppose $\mathcal{A}(B^0, t_0)$ is defined as above, i.e. $B^0 = [b_{ij}]$, where each $b_{ij} = \pm a_{ij}$ and (a_{ij}) is the Cartan matrix of a finite root system Φ . Equivalently, the diagram (resp. quiver) defining $\mathcal{A}(B^0, t_0)$ is an orientation of a (simply-laced) finite type Dynkin diagram. Let D denote the set of all denominator vectors of cluster variables in $\mathcal{A}_{\bullet}(B^0, t_0)$ which do not occur in the initial cluster. Let $S = \{\alpha_1, \ldots, \alpha_n\}$ be the set of simple roots of the corresponding root system Φ and let Φ_+ be the set of positive roots of Φ . There is a bijective correspondence between these cluster variables in \mathcal{A} and the positive roots in Φ_+ . More specifically, if a cluster variable corresponds to $\alpha = \sum d_i \alpha_i$, then the denominator vector of the cluster variable is $(d_1, \ldots, d_n) \in \mathbb{Z}_{\geq 0}^n$.

Recall that we are working with type D_n cluster algebras, so we focus on the associated root system of type D_n . Namely, let Φ_+ be the set of positive roots given by

$$\Phi_{+} = \{e_i + \dots + e_i : 0 \le i \le j \le n-1\} \cup \{e_i + \dots + e_{n-3} + e_{n-1} : 0 \le i \le n-3\}$$

$$\cup \{e_i + \dots + e_{j-1} + 2e_j + \dots + 2e_{n-3} + e_{n-2} + e_{n-1} : 0 \le i < j \le n-3\}.$$

The data of a positive root $\underline{d} = (d_0, \dots, d_{n-1}) \in \Phi_+$ will be included in our definitions for our graph theoretic interpretation of the F-polynomial.

3 Our Model

In this section, we describe our combinatorial model for how to obtain the F-polynomial associated to a type D_n cluster algebra where the associated quiver is acyclic. Our model assigns a graph comprised of one hexagon and n-1 squares to a given quiver where we attach these tiles based on the orientation of each arrow in the quiver. Relying on a bijection between denominator vectors of cluster variables and positive roots in a type D_n root system, we use the data of the quiver Q and a positive root \underline{d} to assign a mixed dimer configuration to this graph. From this assignment, we create a poset of mixed dimer configurations each of which corresponds to a monomial of the F-polynomial associated to \underline{d} and whose coefficient is given by the number of cycles appearing in the mixed dimer configuration.

3.1 Type A Case: Snake Graphs

We model our approach off of the snake graphs for type A_n cluster algebras. This can be viewed as a special case of positive formulas for cluster variables associated to arcs in (unpunctured) surfaces [MS10, MSW11]. We also note [Pro05, Section 2-4] describing unpublished work of Carroll-Price during an REU advised by Jim Propp.

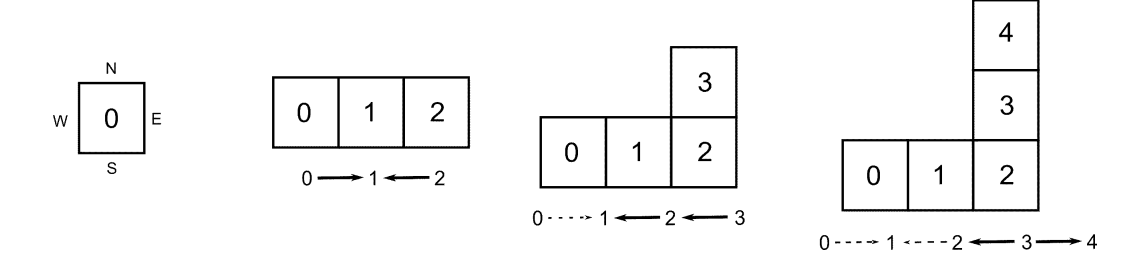
In particular, for an acyclic type A_n quiver, i.e. an orientation of the line segment on n vertices, we can build a bipartite planar graph by adjoining square tiles together. Inductively, an arrow $i \to (i+1)$ or $i \leftarrow (i+1)$ corresponds to adding a tile to the current snake graph to the North or East of the preceding tile, as described by the following rule: when two consecutive arrows are in the same direction, i.e. $(i-1) \to i \to (i+1)$ or $(i-1) \leftarrow i \leftarrow (i+1)$, the corresponding tiles are placed so that they zig-zag (i.e. North then East, or East then North). On the other hand, when two consecutive arrows are in opposite directions, the corresponding tiles are placed straight (i.e. North then North, or East then East). The first step of the snake graph (i.e. the placement of the second tile) may be taken arbitrarily although we conventionally take this as a step to the East, without loss of generality.

Furthermore, we can color the vertices black and white so that for the edge at the border of tiles i and (i+1), if we draw the arrow $i \to (i+1)$ or $i \leftarrow (i+1)$ perpendicular to this edge, then the white vertex appears on the right.

Example 19. Consider the A_5 quiver given by

$$Q = 0 \longrightarrow 1 \longleftarrow 2 \longleftarrow 3 \longrightarrow 4.$$

By the rules described above, this orientation of the A_5 quiver yields the following snake graph on 5 square tiles.

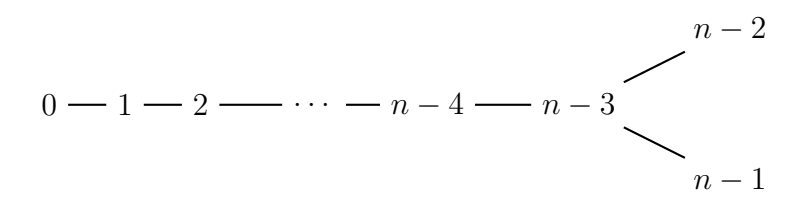


Note the diagram is split up by the inductive process of stacking tiles on the North or East edge of the previous tile. The subquivers are placed below each snake graph where the arrows are bolded in the quiver that dictate the inductive rule for stacking.

In the ensuing subsection, we extend this procedure to acyclic quivers of type D_n , which leads to a single hexagonal tile in addition to the usual square tiles.

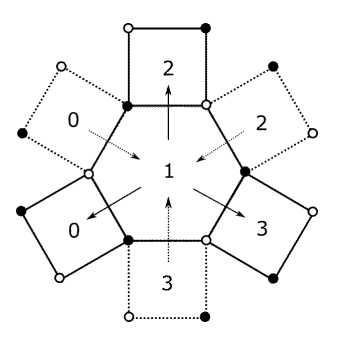
3.2 Obtaining a Hexagon-Square Graph from a Quiver

Consider the Dynkin diagram of type D_n where we agree to associate the labels $0, 1, \ldots, n-1$ to the vertices of the diagram such that the unique degree 3 vertex is labeled n-3.



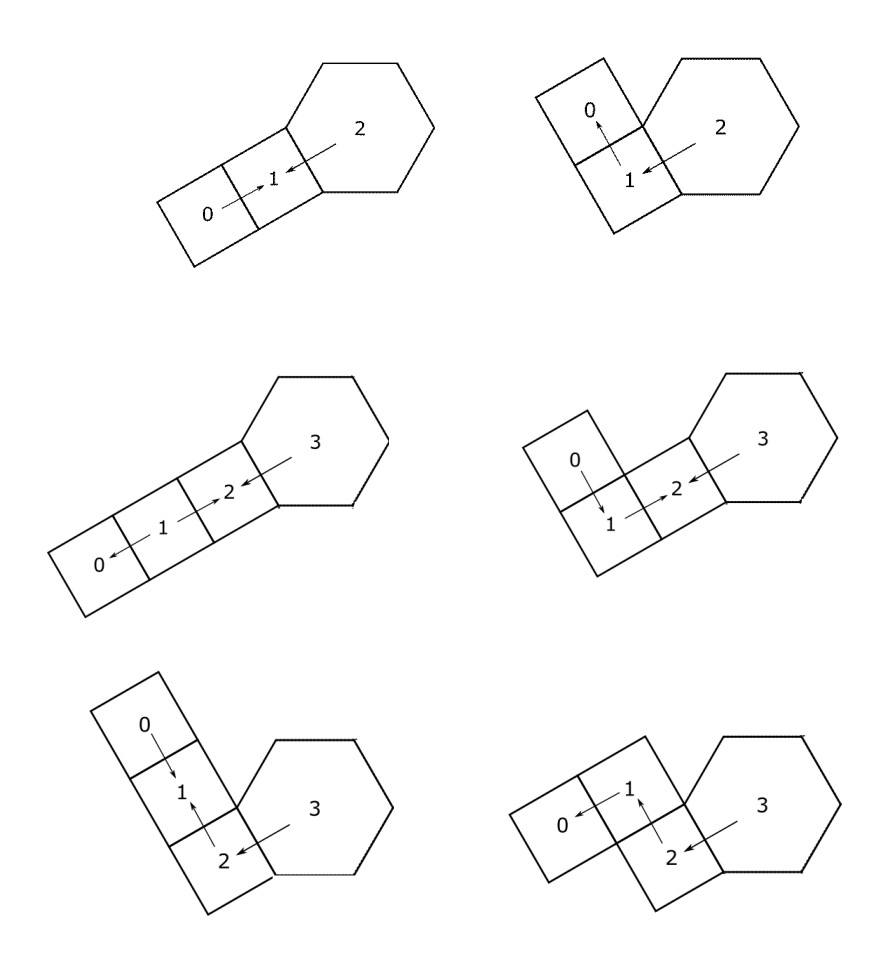
We turn this Dynkin diagram into an acyclic quiver of type D_n by assigning an orientation to each edge of the diagram. We now associate a graph to Q we call the **base graph**, by associating either a square tile or hexagon tile to each vertex in Q. Then, we attach these tiles based on rules dictated by the orientation of the arrow connecting the vertices [PW18].

The unique trivalent vertex labeled n-3 corresponds to the unique hexagon tile in our graph. The rest of the vertices in Q are assigned square tiles. For the case when n=4, all vertices are incident to the trivalent vertex n-3, so we attach the square tiles to the hexagon based on the orientation of the arrow in Q. Note that the base graph, by construction, is a planar bipartite graph. Hence, there are two choices for a black and white coloring on the vertices of the base graph. We adopt the convention that if $i \to j$ in the quiver Q, we "see white on the right." For example, the 8 possible acyclic quivers of type D_4 are illustrated superimposed below, with the associated base graphs similarly superimposed.



Using the fact, for $n \ge 4$, that an acyclic D_n quiver contains an acyclic A_{n-3} subquiver induced on vertices $\{0, 1, 2, \ldots, n-4\}$, we build the usual type A snake graph via square tiles, and include this snake graph as an induced subgraph of our base graph.

From this point forward, when we refer to the base graph, we implicitly take it with this bipartite coloring. When $n \ge 5$, to attach the remaining tiles, we adopt the type A snake graph convention as described in Section 3.1. Below we illustrate some of the possible base graphs for n = 5 and 6. To limit the number of cases, we omit the square tiles associated to (n-2) and (n-1), and assume without loss of generality that the quiver contains the arrow $(n-3) \to (n-4)$ rather than its opposite.

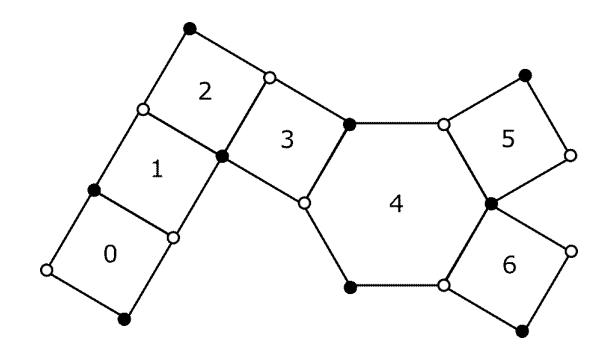


Definition 20. Given a quiver Q of type D_n where the associated quiver is acyclic, the hexagon-square of Q obtained from the above process is called the **base graph** of Q.

Example 21. Suppose we have the following D_7 quiver:

$$Q = 0 \longrightarrow 1 \longleftarrow 2 \longleftarrow 3 \longrightarrow 4$$

By definition of the base graph, mimicking the construction in Example 19, the associated hexagon-square graph is:

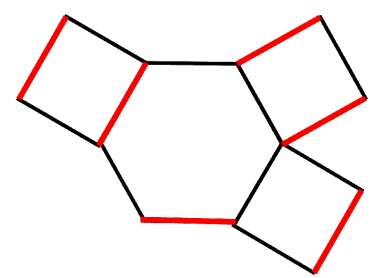


3.3 Associating a Minimal Mixed Dimer Configuration to the Base Graph

For the following definitions, suppose that G is a planar bipartite graph.

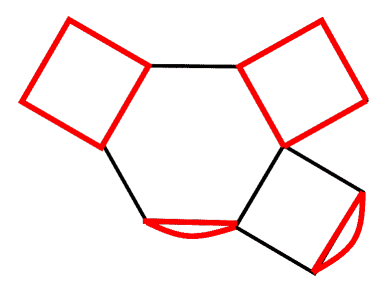
Definition 22. A dimer configuration (also known as a matching) is a subset $D \subset E(G)$ such that every vertex $v \in V(G)$ is contained in exactly one edge $e \in D$.

For example, consider the red edges in the following graph:

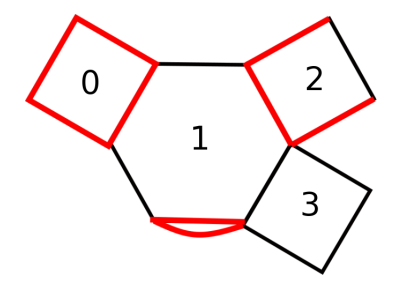


Definition 23. A double dimer configuration D' of G is a multiset of the edges of G such that every vertex $v \in V(G)$ is contained in exactly two edges $e, e' \in D'$.

For example, consider the red edges in the following graph:



Now, we aim to associate a "mixed dimer configuration" to the base graph obtained in the previous section which, as the name suggests, is a mixture between a dimer configuration and a double dimer configuration. For example, consider the red edges in the following graph:



In order to define mixed dimer configurations that satisfy a certain "valency condition," we need to introduce another piece of global data other than the quiver Q.

Definition 24. Let \underline{d} be an n-tuple whose entries are each 0, 1, or 2, i.e. $\underline{d} \in \{0, 1, 2\}^n$. A **mixed dimer configuration** M of G is a multiset of the edges of G such that every vertex $v \in V(G)$ is contained in zero, one, or two edges in M. Furthermore, we say that M satisfies the **valence condition** with respect to d if

- Each vertex incident to a tile labeled i with $d_i = 2$ is contained in two edges in M.
- Each vertex incident to a tile labeled i with $d_i = 1$ is contained in at least one edge in M.

For example, in the above toy example of a mixed dimer configuration, the associated 4-tuple would be $\underline{d} = (2, 2, 1, 0)$. Motivated by denominator vectors of cluster variables for cluster algebras of type D_n , i.e. of finite type, we focus on the special case where \underline{d} is a positive root of the root system of type D_n , which we denote as Φ .

3.3.1 Defining the minimal mixed dimer configuration M_{-}

Fix some type D_n quiver Q where the associated quiver is acyclic and let $\underline{d} \in \Phi_+$. Let G be the associated base graph with fixed bipartite coloring. For all the entries $d_i \geq 1$, consider the induced subgraph $G_1 \subset G$ using the associated tiles i for $0 \leq i \leq n-1$. Traversing around the boundary of G_1 clockwise, distinguish the edges that go from black

to white in the bipartite coloring which should notably result in a dimer configuration of G_1 , call it M_1 .

We remark that this is well-defined because the subgraph $G_1 \subset G$ is connected due to the structure of the root $\underline{d} \in \Phi_+$, i.e. all of the positive entries appear such that the tiles in G associated to them are neighboring.

Next, for all the entries $d_j = 2$, consider the induced subgraph $G_2 \subset G_1 \subset G$ using the associated tiles j for $0 \leq j \leq n-1$. Going around the boundary of G_2 clockwise, distinguish the edges that go from black to white in the bipartite coloring which should notably result in a dimer configuration of G_2 , call it M_2 .

Again, we remark that this is well-defined because the subgraph $G_2 \subset G$ is connected due to the structure of the root $\underline{d} \in \Phi_+$.

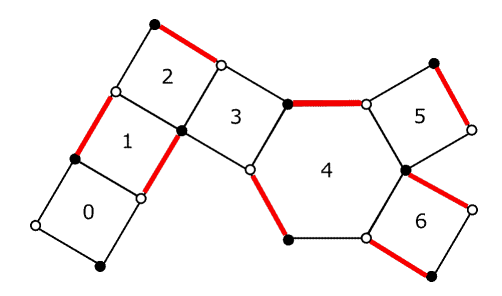
Taking the superimposition of M_1 and M_2 , we have some multiset of the edges of our base graph G. At this stage, the valence¹ of each vertex in either 0, 1, or 2 in $M_1 \sqcup M_2$. In particular, for every vertex $v \in G$, we insist the valence of v in $M_1 \sqcup M_2$ is the maximal value of d_i , for i in the set of labels for tiles incident to vertex v. In particular, the mixed dimer configuration $M_1 \sqcup M_2$ constructed in this way satisfies the valence condition with respect to d, as defined in Definition 24.

Definition 25. The minimal mixed dimer configuration associated to the bipartite planar base graph G and to the type D_n positive root $\underline{d} = (d_0, \ldots, d_{n-1}) \in \Phi_+$ is given by

$$M_{-}(Q,\underline{d}) := M_1 \sqcup M_2.$$

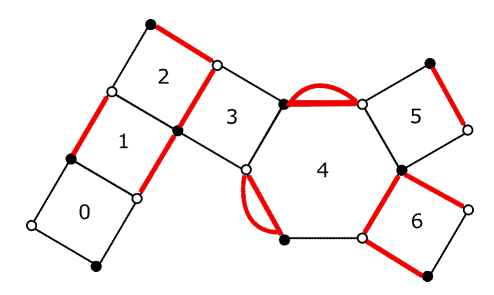
For brevity, we denote the minimal mixed dimer configuration by $M_{-} := M_{-}(Q,\underline{d})$. Sometimes we will instead use the term **minimal matching** for M_{-} . We illustrate this process via an example.

Example 26. Consider the quiver in Example 2.1 and take the positive root $\underline{d} = (0, 1, 1, 2, 2, 1, 1)$. Then, the graph G_1 will consist of all the tiles except the tile 0, as $d_0 = 0$. When enumerating the boundary edges of G_1 oriented black to white clockwise, we obtain M_1 :



¹Here, and from now on, when we refer to the "valence" of a vertex, we refer to the valence with respect to a mixed dimer configuration rather than the valence of the vertex in the base graph.

Since $d_3 = d_4 = 2$, we have that the graph G_2 contains tiles 3 and 4. So, we distinguish a double dimer configuration on these tiles by traversing the boundary of tiles 3 and 4 and enumerating the edges that are oriented black to white clockwise. If one of these edges was distinguished in the previous step, distinguish it again with a doubled edge. We obtain $M_-(Q, d) = M_1 \sqcup M_2$:

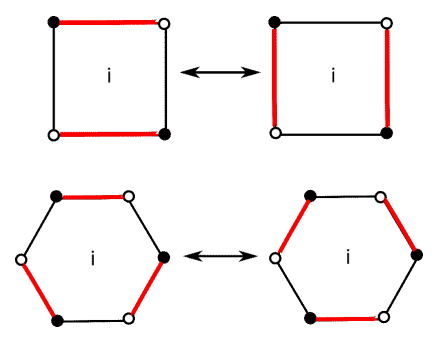


This is the minimal matching associated to Q and \underline{d} .

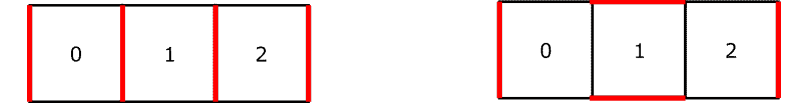
3.4 Poset of Mixed Dimer Configurations

We now create the poset of mixed dimer configurations where each of the mixed dimer configurations appearing in this poset corresponds to a monomial that appears in the F-polynomial associated to \underline{d} . In order to define this poset, we first define a larger poset, and then refine its set of elements to obtain the poset which we desire.

The poset relation we will define is inspired by flips of tiles in dimer configurations, in the sense of [KW10] and [MS10]. This local operation is classically given by:

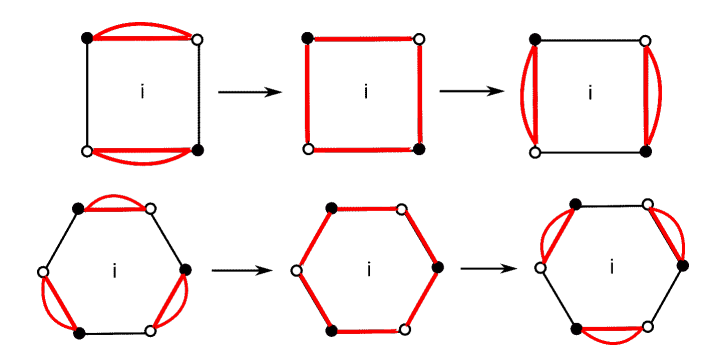


Remark 27. Not all tiles in a given dimer configuration can be flipped. Consider the following example:



In the left dimer configuration, we can flip every tile 0, 1, and 2 from the vertical configuration to the horizontal configuration. However, in the right dimer configuration, the only tile we can flip is tile 1, i.e. by replacing the horizontal configuration with the vertical configuration. We cannot flip tile 0 because the edge straddling tile 0 and 1 is not present in this configuration. Similarly, we cannot flip tile 2.

To extend this to a mixed dimer configuration, we define flipping as moves that we can perform twice in a row on tiles:



Remark 28. This modification is necessary to model the F-polynomial in type D because there are monomials that appear with terms with an exponent of two i.e. a term like u_i^2 . In the type A case, no such exponent of two appears which meant that the dimer configurations where flipping is an involution was sufficient.

Definition 29. We say that the flip of tile i is **allowable** if we can flip tile i as in the pictures shown above. More concretely, if all edges going black to white clockwise occur in a mixed dimer configuration on tile i, we can exchange these edges for the edges that go white to black clockwise. If for a given edge of the graph, there are multiple copies of that edge in a mixed dimer configuration, then with each flip, we only exchange a single copy of that edge. Implicit in this definition is that the associated d_i is positive.

Definition 30. Let (\bar{P}, \leq) be the **poset of mixed dimer configurations** that satisfy the valence condition and are reachable via a sequence of allowable flips from $M_{-}(Q, \underline{d})$. For two such mixed dimer configurations D and D', we say that $D \leq D'$ if there exists a sequence of allowable flips from D to obtain D'.

The poset \bar{P} turns out to have more elements than the number of monomials in the F-polynomial associated to \underline{d} . Hence, we need to refine the number of elements in our poset by disallowing some sequences of allowable flips. We will let $(P, \leq) \subseteq (\bar{P}, \leq)$ be the subposet of mixed dimer configurations that satisfy the valence condition, are reachable via a sequence of allowable flips from M_- , and satisfy the following condition known as being **node monochromatic**.

3.4.1 Node Monochromatic Mixed Dimer Configurations

Fix a type D_n quiver Q and a positive root $\underline{d} = (d_0, \ldots, d_{n-1}) \in \Phi_+$. Let G be the associated base graph with fixed bipartite coloring. We now define a condition required of mixed dimer configurations to model the F-polynomial.

We distinguish three pairs of vertices of G that we call **nodes** via the following prescription:

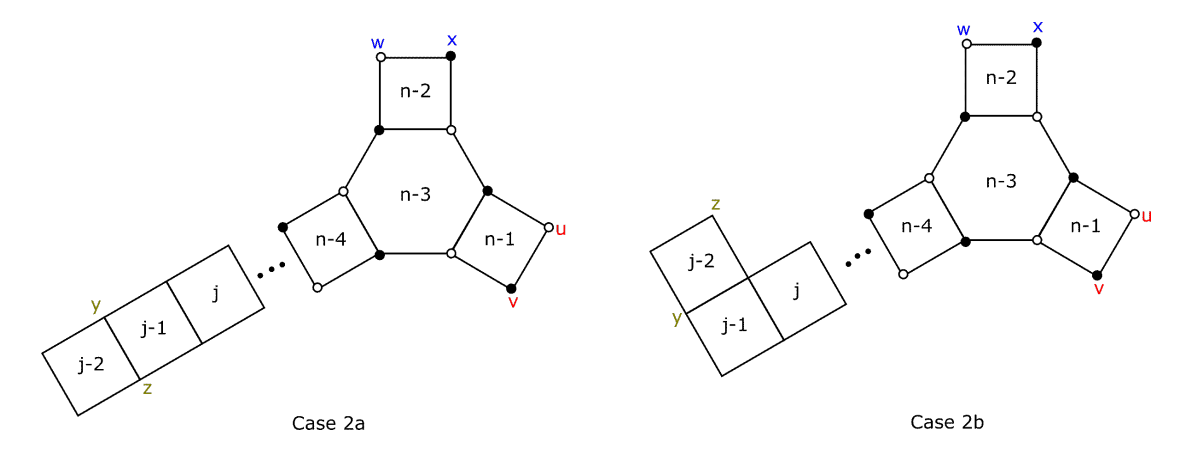
- On the tile labeled n-1, take the two vertices of the square tile that are not incident to the hexagon, call them $u, v \in V(G)$. Color these nodes u, v red.
- On the tile labeled n-2, take the two vertices of the square tile that are not incident to the hexagon, call them $w, x \in V(G)$. Color these nodes w, x blue.
- The last choice of vertices splits into a few cases. Let d_j be a 2 in the positive root d of minimal index.

Case 1: If j-2 < 0, then this means that j=1. Take the two vertices on tile 0 that are not incident to tile 1, call them $y, z \in V(G)$. Color these nodes y, z green.

Case 2: Suppose $j \ge 2$. We now have two subcases.

- Case 2a. If the tiles j-2, j-1, j are placed straight, i.e. the orientation in the quiver is given by $j-2 \to j-1 \leftarrow j$ or $j-2 \leftarrow j-1 \to j$, we take the two vertices on tile j-1 that are not incident to tile j, call them $y, z \in V(G)$.
- Case 2b. If the tiles j-2, j-1, j are placed in a zig-zagging fashion, i.e. the orientation in the quiver is given by $j-2 \leftarrow j-1 \leftarrow j$ or $j-2 \rightarrow j-1 \rightarrow j$, we choose y on tile j-1 as the vertex belonging to the edge that is incident to tile j-2, but not tile j. We choose z on tile j-2 that is "diagonally across" from y. Color these nodes y, z green. In the two figures (above and below), we illustrate our definition of the green nodes.

The placement of the green nodes is illustrated in the following figure:²



Definition 31. A mixed dimer configuration M of G is **node-monochromatic** if any path consisting of edges in M between nodes connects nodes of the same color. If there exists a path consisting of edges in M between nodes of different colors, we say M is **node-polychromatic**.

²Note that to make these diagrams as clear as possible, we have fixed an orientation of the arrows between n-1, n-2 and n-1, n-3 as we previously defined the red and blue nodes. We have also fixed an orientation between n-3 and n-4 as it does not affect the definition of the green nodes.

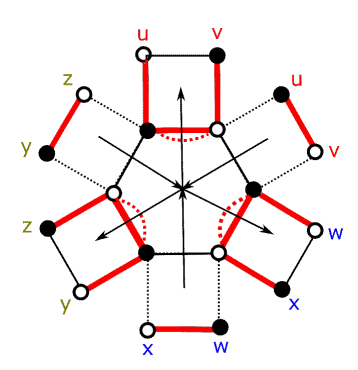
Remark 32. We note that if $\underline{d} \in \{0,1\}^n$, i.e. \underline{d} does not contain a 2, then any mixed dimer configuration satisfying the valence condition given by \underline{d} is always node-monochromatic. To see this most easily, we observe that such a mixed dimer configuration is a perfect matching on the subgraph defined by the support of \underline{d} , but the distance between any two nodes of different colors is at least two.

Remark 33. Our definition of node-monochromatic dimer configurations in Definition 31 differs from the rules appearing in related research on weighted enumeration of double dimer configurations such as in Jenne's work [Jen19] or in Kenyon-Wilson's work [KW10] in the following way. In [Jen19] or [KW10], the set of nodes is divided into three circularly contiguous sets R, G, and B in such a way so that no node is paired with a node in the same set. In our model, we also have nodes colored by three circularly continguous sets, but being node-monochromatic requires (rather than forbids) the endpoints of a path are of the same color.

Now that the poset P is well-defined, we aim to show that the minimal matching is in this poset.

Proposition 34. M_{-} is in P, i.e. is a mixed dimer configuration on the base graph that satisfies the valence condition and is node-monochromatic.

Proof. First note that M_{-} trivially satisfies the condition that it is reachable by a sequence of allowable flips from M_{-} by taking the empty sequence. Note that M_{-} also satisfies the valence condition by construction. So, it suffices to show that M_{-} is node-monochromatic by showing that there are no paths between nodes of different colors. This is a consequence of the bipartite coloring. By a case-by-case analysis for the acyclic orientations of quivers of type D_4 , we see that no nodes of different colors can be connected in any orientation of the quiver. The following diagram represents all 8 acyclic orientations of D_4 drawn on one graph where the choice of orientation of arrow in the quiver is indicated on top of the graph:



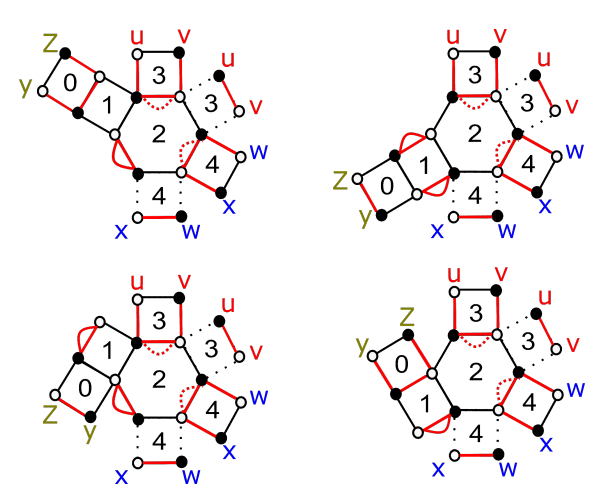
By the definition of M_{-} , for any n, the longest path distinguished in the matching has length 3. This occurs because when enumerating the dimer configuration in G_1 , we only create paths of length 1. When enumerating edges in G_2 , we distinguish all clockwise black to white oriented edges on the boundary of G_2 . If these edges are also boundary edges of G_1 , then we create a 2-cycle on these edges. If these edges were not boundary

edges of G_1 , they must be interior edges of G_1 in which case their inclusion creates a path of length 3 as enumerating this interior edge connects two boundary edges that were previously distinguished.

Suppose that two nodes of different colors can be connected by a path of length 2 in G. (Note that no path of length 1 can connect nodes of different colors by definition.) In this case, it suffices to look at D_4 , as with higher D_n , the nodes y, z move farther away from the other nodes and cannot be connected by a path of length 2. Both edges in this path of length two must be boundary edges of G, i.e. edges that do not straddle two different tiles in G. Moreover, with respect to the full graph G, one is colored black to white clockwise and the other must be colored white to black clockwise. By definition of M_- , we do not distinguish boundary edges that are oriented white to black clockwise. So, only the edge oriented black to white clockwise will appear in M_- which means that this path cannot be contained in M_- .

Now suppose that there is a path of length 3 in G connecting nodes of different colors. In this case, it suffices to look at D_5 , as with higher D_n , the nodes y, z move farther away from the other nodes and cannot be connected by a path of length 3. In order to connect nodes of different colors, this path would have to traverse over a white to black clockwise edge on the boundary of G_2 . This is because in any orientation of D_5 , paths cannot be formed using the white to black clockwise oriented edges with respect to the hexagon in M_- .

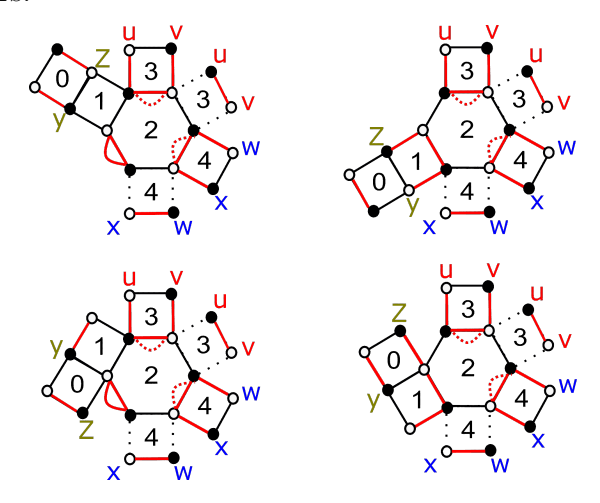
For D_5 , there are two positive roots that make it potentially possible for nodes of different color to be connected; either $\underline{d} = (1, 2, 2, 1, 1)$ or $\underline{d} = (1, 1, 2, 1, 1)$. The following diagram represents the minimal matching when $\underline{d} = (1, 2, 2, 1, 1)$, i.e. Case 1 in Section 3.4.1. In all possible orientations of D_5 , paths in M_- do not connect nodes of different colors³.



The next diagram represents the minimal matching when $\underline{d} = (1, 1, 2, 1, 1)$ i.e. Cases

 $^{^3}$ Just like in the D_4 case above, we superimpose together the various possible base graphs for D_5 , but use dotted edges to illustrate the contrasts.

2a and 2b in Section 3.4.1. In all possible orientations of D_5 , paths in M_- do not connect nodes of different colors.



So, by definition of M_{-} , no boundary white to black clockwise edge is distinguished in G_2 which means this path cannot be contained in M_{-} . Thus, M_{-} is node-monochromatic.

We show that the elements in (P, \leq) give the nonzero monomials in the F-polynomial associated to \underline{d} .

3.5 Main Theorem

Theorem 35. Given an acylic quiver Q of type D_n and a choice of positive root $\underline{d} \in \Phi_+$ for the corresponding root system, we let $F_{\underline{d}}$ denote the F-polynomial corresponding to the cluster variable with denominator vector \underline{d} . This expression is based on the appropriate cluster algebra of type D_n and assuming an initial seed defined by the choice of quiver Q and the standard initial cluster of $\{x_1, x_2, \ldots, x_n\}$.

Furthermore, let $M_- = M_-(Q,\underline{d})$ be the minimal matching, as defined in Section 3.3.1 and let P be the poset of mixed dimer configurations that satisfy the valence condition, are reachable via a sequence of allowable flips from M_- , and satisfy the node monochromatic condition. Then the expansion of F-polynomial $F_{\underline{d}}$ can be expressed as a weighted multivariate rank-generating function on the poset (P, \leq) determined by M_- :

$$F_{\underline{d}} = \sum_{D \in P} 2^{c} u_0^{t_0} u_1^{t_1} \cdots u_{n-1}^{t_{n-1}},$$

where the sum is taken over mixed dimer configurations D obtained by flipping tile i t_i -times (keeping track of multiplicities) and c is the number of cycles enclosing a face in D.

We provide an example before proceeding to the proof of Theorem 35.

Example 36. Suppose that we have the following D_6 quiver:

$$Q = 0 \longleftarrow 1 \longleftarrow 2 \longleftarrow 3$$
5

Suppose that we take $\underline{d} = (1, 1, 2, 2, 1, 1) \in \Phi_+$. Then, we have that the F-polynomial associated to \underline{d} is given by:

$$\begin{split} F_{\underline{d}} &= 1 + u_0 + u_2 + u_5 + u_0 u_1 + u_0 u_2 + u_0 u_5 + u_2 u_5 \\ &+ 2 u_0 u_1 u_2 + u_0 u_1 u_5 + u_0 u_2 u_5 + u_2 u_3 u_5 + 2 u_0 u_1 u_2 u_5 + u_0 u_1 u_2^2 \\ &+ u_0 u_1 u_2 u_3 + u_0 u_2 u_3 u_5 + 2 u_0 u_1 u_2 u_3 u_5 + u_0 u_1 u_2^2 u_5 + u_0 u_1 u_2^2 u_3 \\ &+ u_0 u_1 u_2 u_3 u_4 u_5 + 2 u_0 u_1 u_2^2 u_3^2 u_5 + u_0 u_1 u_2^2 u_3 u_4 u_5 + u_0 u_1 u_2^2 u_3^2 u_5 + u_0 u_1 u_2^2 u_3^2 u_4 u_5 \end{split}$$

The poset P is Figure 1 on the following page where tiles are shaded grey to emphasize when they have been enclosed by a cycle.

Remark 37. We see that we do not flip at all tiles at which we can perform allowable flips. It is crucial that these mixed dimer configurations stay node-monochromatic. For example, if we analyze the set of allowable flips from the minimal matching M_{-} , after flipping tile 2, an allowable flip can occur at the hexagon, tile 3. However, the monomial u_2u_3 does not appear in F_d . With our choice of nodes, we see that by flipping tile 3, we connect nodes of different colors i.e. there is a path between the green node z to the red node v. This is why the mixed dimer configurations in our poset must be node-monochromatic. In Section 3.6, we show a poset-theoretic consequence of this restriction.

3.6 The poset of node-monochromatic mixed dimer configurations is not distributive

After defining our poset of (node-monochromatic) mixed dimer configurations, which we denoted as (P, \leq) , it is of independent combinatorial interest to investigate its properties. Our poset of mixed dimer configurations forms a lattice since the unique minimal element corresponds to the constant term 1 in the F-polynomial and the unique maximal element corresponds to u^d in the F-polynomial.

Recall a lattice is distributive if the operations of meet and join distribute over one another i.e. for any $A, B, C \in P$, we have

$$A \vee (B \wedge C) = (A \vee B) \wedge (B \vee C).$$

In the Type A case, Theorem 5.2 in [MSW13], based on [Pro02, Section 3], states that the snake graph poset of perfect matchings form a distributive lattice. It turns out that this is not the case for our poset of mixed dimer configurations as it contains a forbidden sublattice⁴ on 5 vertices that form a pentagon shape. Consider the following counterexample deduced from Figure 13:

⁴On this sublattice, we have the property that the meets and joins of pairs of elements agree with their images as they would be in the original lattice.

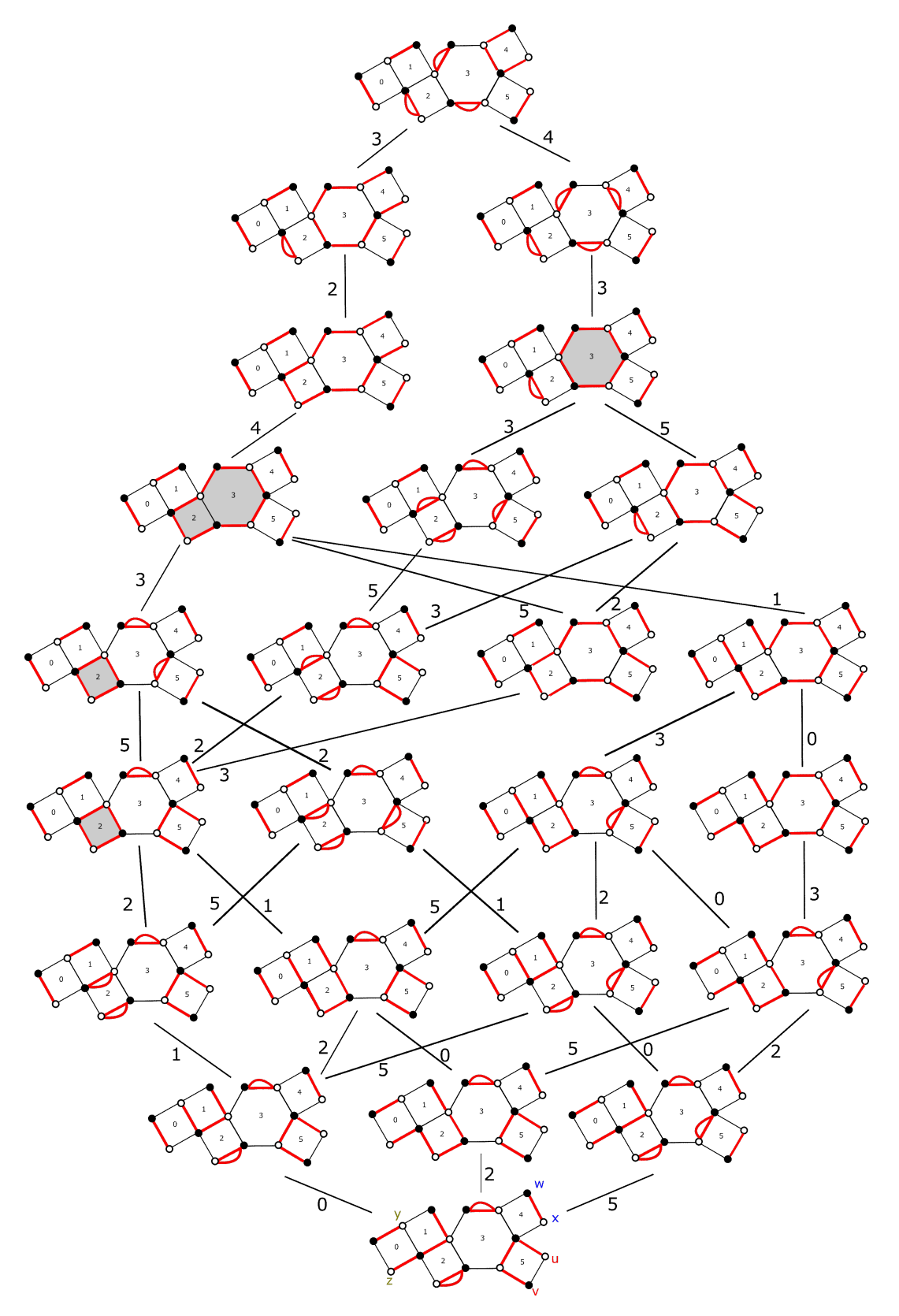
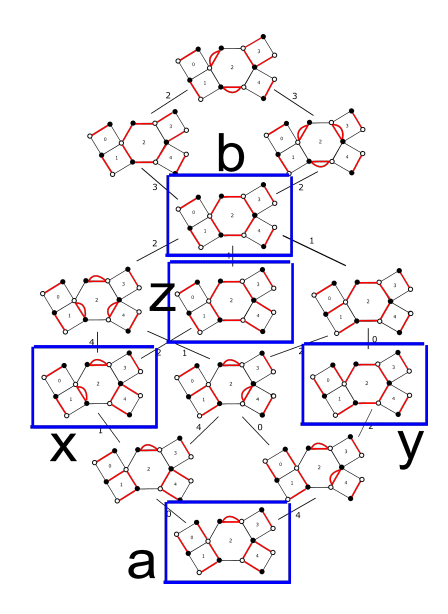


Figure 1 – The poset associated to Example 36.



Note that $x \vee (y \wedge z) = x$ whereas $(x \vee y) \wedge (x \vee z) = z$, Hence, our poset of mixed dimer configurations fails to be distributive.

4 Proof of Theorem 35

In order to prove that this mixed dimer configuration model indeed gives the F-polynomial, we construct bijections between mixed dimer configurations and tuples of integers which come from a model of Thao Tran [Tra09].

4.1 Thao Tran's Model

Define a partial order \geq on \mathbb{Z}^n via

$$\underline{a} \geqslant \underline{a}'$$
 if $\underline{a} - \underline{a}' \in \mathbb{Z}_{\geq 0}^n$.

Definition 38. [Tra09, Definition 4.1] Fix $n \ge 4$, and let Q denote an acyclic quiver of type D_n . Further, fix $\underline{d} \in \Phi_+$, a positive root of type D_n , and $\underline{e} = (e_0, \dots, e_{n-1}) \in \mathbb{Z}^n$ with $0 \le \underline{e} \le \underline{d}$. An arrow $i \to j$ in Q is **acceptable** with respect to the pair $(\underline{e}, \underline{d})$ if

$$e_i - e_j \leq \max(d_i - d_j, 0).$$

An arrow $i \to j$ is **critical** with respect to the pair $(\underline{e},\underline{d})$ if either

$$(d_i, e_i) = (2, 1)$$
 and $(d_i, e_i) = (1, 0)$

or

$$(d_i, e_i) = (1, 1)$$
 and $(d_j, e_j) = (2, 1)$.

Let S be the induced subgraph of Q on the set of vertices $\{i : (d_i, e_i) = (2, 1)\}$. For a connected component C of S, define

 $\nu(C) = \#\{\text{critical arrows having a vertex in } C\}.$

Theorem 39. [Tra09, Theorem 4.2] Fix $\underline{d} \in \Phi_+$, $\underline{e} \in \mathbb{Z}^n$. For the cluster algebra defined by the initial quiver Q (acyclic of type D_n), the coefficient of the monomial $u_0^{e_0} \cdots u_{n-1}^{e_{n-1}}$ in the F-polynomial associated to \underline{d} is nonzero if and only if all of the following conditions, which we refer to as **Tran's conditions** in the sequel, are satisfied:

- 1. $0 \leqslant e \leqslant d$
- 2. all arrows in Q are acceptable
- 3. $\nu(C) \leq 1$ for all connected components C of S, where S is the induced subgraph as defined above.

The coefficient of $u_0^{e_0} \cdots u_{n-1}^{e_{n-1}}$ is 2^c , where c is the number of connected components C such that $\nu(C) = 0$.

Remark 40. Although [Tra09] proves Theorem 39 in more generality, i.e. for other Dynkin types, we focus on her proof in case of Type D_n quivers. For this, she utilizes [Tra09, Theorem 4.7], whose proof involves the Quiver Grassmanian, denoted $Gr_{\underline{e}}(M)$, which is the variety of all subrepresentations of a quiver representation M of dimension \underline{e} . It is a closed subvariety of a product of Grassmannians. Her proof involves computing the F-polynomial by calculating Euler-Poincaré characteristics for multiple quiver Grassmannians ranging over various vectors \underline{e} , relying on [DWZ10] for the correspondence between these two objects. To compute the Euler-Poincaré characteristic of $Gr_{\underline{e}}(M)$, Tran shows that conditions (1), (2), and (3) exactly give subrepresentations of dimension \underline{e} for which the corresponding Euler-Poincare characteristic is nonzero. This provides the computation of the support of the F-polynomial.

4.2 Bijection of Models

4.2.1 Monomials

Theorem 41. Let Q be an acyclic quiver of type D_n and let $\underline{d} \in \Phi_+$. There is a bijection between

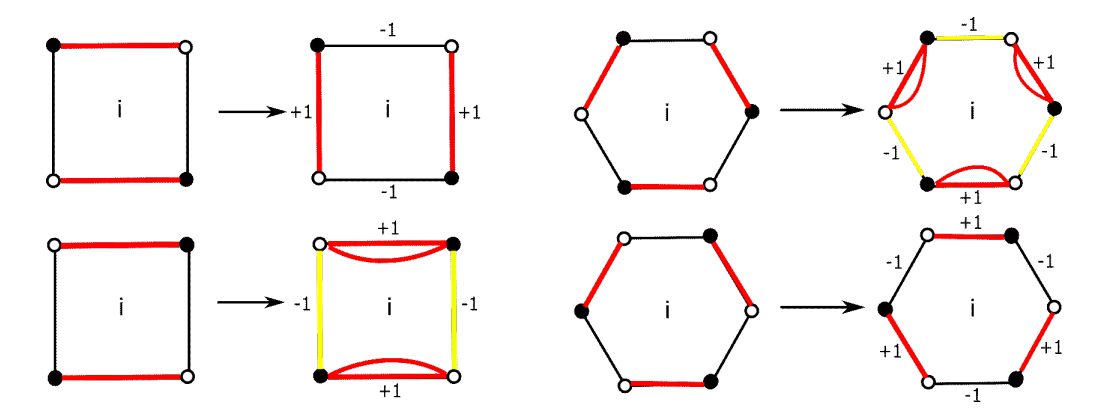
 $\{mixed\ dimer\ configurations\ D\ in\ P\} \stackrel{\sim}{\longleftrightarrow} \{vectors\ \underline{e}\ satisfying\ Tran's\ conditions\}.$

This bijection is described as a map in both directions. The map sending $\underline{e} \longrightarrow D$ is given by performing a particular set of flips from M_{-} . In order to describe this direction of the bijection, we weight the edges of the base graph G (which is associated to some quiver Q and positive root \underline{d}) via

$$w(e) := \#\{ \text{ edges on } e \text{ in } M_- \}$$

for all $e \in E(G)$.

Definition 42. The weights of the edges are transformed via the following prescription after flipping a tile:



This is known as a **weighted flip**.

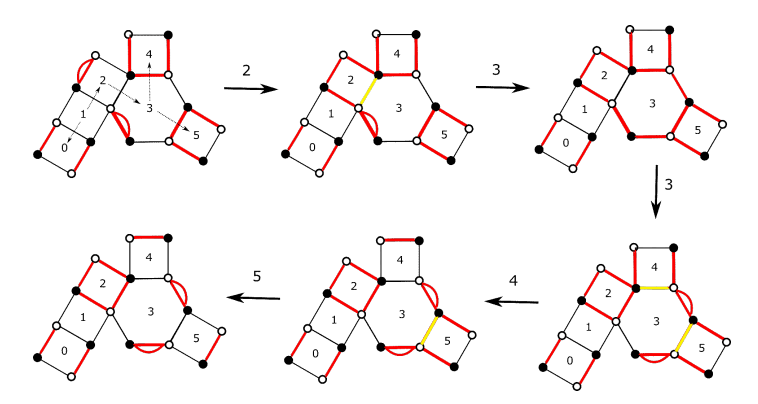
Remark 43. Implicit in this definition is the fact that our weights will stay non-negative when we perform what we have previously called "allowable flips." However, in the context of this direction of the bijection, we will allow for weighted flips at any tile; meaning that we now allow the weight of an edge to be negative. To emphasize the deficits which arise when we flip edges that we previously could not in the "allowable" sense, we distinguish edges of negative weight in yellow and call them "antiedges." By introducing these weights and allowing them to be negative, we simplify the noncommutativity of flipping sequences of tiles.

Theorem 44. Given $(Q,\underline{d},\underline{e})$ where \underline{e} satisfies Tran's conditions, i.e. (1), (2), and (3) of Theorem 39, there exists a unique mixed dimer configuration D in poset P (see Section 3.4) such that D is associated to this \underline{e} . Further, the mixed dimer configuration D is obtained by the following procedure:

- 1. Given (Q,\underline{d}) , construct the corresponding base graph G and the minimal matching M_{-} associated to \underline{d} via the procedure described in Section 3.2. Weight the edges of G by w(e) for $e \in E(G)$.
- 2. From this weighted minimal matching, take the positive entry $e_{i_1} > 0$ in \underline{e} of minimal index. Flip tile i_1 e_{i_1} number of times and transform its edge weights as prescribed in Definition 42 with respect to the black and white coloring of the vertices to arrive at the mixed dimer configuration D_1 . (Note that if this flip (or flips) were not "allowable," then we will obtain "antiedges", i.e. edges with negative weight we highlight in yellow.)
- 3. From D_1 , take the next positive entry $e_{i_2} > 0$ in \underline{e} of minimal index. Flip tile i_2 e_{i_2} number of times and transform its edge weights as prescribed in Definition 42 to arrive at the mixed dimer configuration D_2 .
- 4. Iterate this process until we have exhausted all positive entries in <u>e</u>. The resulting mixed dimer configuration D will only have non-negative weights, i.e. no yellow edges will remain. Moreover, it will be an element of P. The resulting configuration D is the mixed dimer configuration associated to <u>e</u>.

Before proving this theorem, we compute an example.

Example 45. Suppose $\underline{d} = (1, 1, 2, 2, 1, 1)$ and Q is superimposed on the first mixed dimer configuration. Let $\underline{e} = (0, 0, 1, 2, 1, 1)$ which we see satisfies conditions (1)-(3) in [Tra09]. Performing the flips in left to right order as prescribed in Theorem 44, we obtain the following sequence of weighted flips



where yellow edges have weight -1 that we refer to as "antiedges" and the last dimer configuration D is the resulting mixed dimer configuration. Note that, in this example, we could flip tiles in the order 3,2,4,5,3 to obtain a sequence of allowable flips yielding D.

In order to prove the above statement, we will utilize the following lemmas:

Lemma 46. Let $\underline{d} \in \Phi_+$ and let $0 \leq \underline{e} \leq \underline{d}$. Suppose that $i \to j$ in Q and for any $0 \leq i \leq n-1$, let D be the mixed dimer configuration obtained by flipping tile i e_i number of times from M_- . Let $m_{i,j}$ be the number of edges distinguished in D on the edge between tiles i and j. Then

$$m_{i,j} = \max(d_i - d_j, 0) + (e_j - e_i) =: n_{i,j}.$$

Proof. In order to prove this formula holds, we proceed by induction on $|\underline{e}| := \sum_{k=0}^{n-1} e_k$. When $|\underline{e}| = 0$, i.e. $\underline{e} = (0, 0, \dots, 0)$, the associated mixed dimer configuration is M_- . By definition of M_- , we distinguish boundary edges in G_1 and G_2 that are oriented black to white clockwise with respect to the bipartite coloring. This means that we only distinguish internal edges when G_1, G_2 are strict subsets of G. Suppose that $d_i > 0$, but $d_j = 0$, i.e. $i \in G_1$ and possibly G_2 whereas $j \notin G_1$ or G_2 . If $i \to j$ in G_2 , then locally we have that the edge straddling i and j is oriented black to white clockwise with respect to the tile i. So, this gives that $m_{i,j} = d_i$ - as we will distinguish this edge in G_1 . If $d_i = 2$, we will distinguish it once again. Therefore, in the case that $i \to j$, we've shown

$$n_{i,j} = \max(d_i - d_j, 0) = d_i = m_{i,j}.$$

If $j \to i$, then we locally have that the edge straddling i and j is oriented white to black clockwise with respect to the tile i. So, this gives that $m_{j,i} = 0$ as we will never distinguish this edge in G_1 or G_2 . Therefore, in the case that $j \to i$, we've shown

$$n_{j,i} = \max(d_j - d_i, 0) = 0 = m_{j,i}$$

Thus, when $|\underline{e}| = 0$, our formula holds. Suppose up to $k \in \mathbb{N}$, we have that when $|\underline{e}| = k$, our formula holds. Now, suppose $|\underline{e}| = k + 1$, and choose $\underline{\tilde{e}}$ with $|\underline{\tilde{e}}| = k$, such that \underline{e} can be derived from $\underline{\tilde{e}}$ by adding 1 to the i^{th} entry of $\underline{\tilde{e}}$. On the level of the mixed dimer configuration, this means we flipped tile i from the mixed dimer configuration associated to $\underline{\tilde{e}}$ to obtain the mixed dimer configuration associated to \underline{e} .

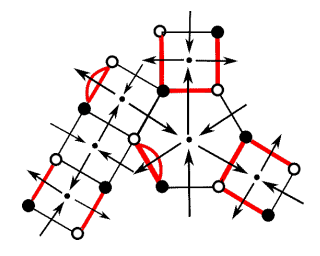
Suppose $i \to j$ in Q. Note that by definition of the weighted flip, we have that the weight of the edge straddling tiles i and j is oriented black to white clockwise on tile i which gives us that the weight decreases by 1. So, we have that $m_{i,j}$ has decreased by 1 and since e_i has increased by 1, we have

$$n_{i,j} = \max(d_i - d_j, 0) + (e_j - (e_i + 1)) = \max(d_i - d_j, 0) + (e_j - e_i) - 1.$$

Therefore, performing a flip at tile i decreased both $n_{i,j}$ and $m_{i,j}$ by 1. If $j \to i$ in Q, the argument is similar.

Corollary 47. The values $n_{i,j} := \max(d_i - d_j, 0) + (e_j - e_i)$ all satisfy $n_{i,j} \ge 0$ if and only if all weights on interior edges on the mixed dimer configuration D associated to e are nonnegative. In particular, all arrows $i \to j$ are acceptable with respect to $(\underline{d}, \underline{e})$ if and only if all weights on interior edges are nonnegative on the mixed dimer configuration D associated to e.

Lemma 48. (Analogous formula to Lemma 46 with boundary edges). Let $\underline{d} \in \Phi_+$ and let $0 \leq \underline{e} \leq \underline{d}$. For any $0 \leq i \leq n-1$, let D be the mixed dimer configuration obtained by flipping tile i e_i number of times from M_- . Let the outer face of our graph G be indexed by ∞ . We assign an arrow to each of the boundary edges of G where the orientation of this arrow depends on the bipartite coloring of G following the convention that we "see white on the right." For example,



We assign a weight to the edge α on tile i as follows:

$$n_{i,\infty}(\alpha) = \max(d_i, 0) - e_i \quad \text{if } i \to \infty \text{ about } \alpha$$

$$n_{\infty,i}(\alpha) = \max(-d_i, 0) + e_i \quad \text{if } \infty \to i \text{ about } \alpha$$

Let $m_{i,\infty}(\alpha)$ (respectively $m_{\infty,i}(\alpha)$) be the number of edges distinguished on α on tile i in D where $i \to \infty$ about α (respectively $\infty \to i$ about α .) Then for any boundary edge α on tile i,

$$n_{i,\infty}(\alpha) = m_{i,\infty}(\alpha)$$
 and $n_{\infty,i}(\alpha) = m_{\infty,i}(\alpha)$.

Proof. The proof is similar to that of Lemma 46.

Remark 49. Note that if we set $(d_{\infty}, e_{\infty}) = (0, 0)$, our formula for the number of boundary edges in Lemma 48 coincides with our formula for the number of internal edges in Lemma 46 as

$$n_{i,\infty}(\alpha) = \max(d_i - d_\infty, 0) + (e_\infty - e_i)$$
 if $i \to \infty$ about α
 $n_{\infty,i}(\alpha) = \max(d_\infty - d_i, 0) + (e_i - e_\infty)$ if $\infty \to i$ about α

Corollary 50. Whenever $0 \le \underline{e} \le \underline{d}$, there are no antiedges on the boundary.

We now prove Theorem 44.

Proof. Let Q be a quiver of type D_n where the associated quiver is acyclic. Let $\underline{d} \in \Phi_+$. Obtain the base graph G(Q) = G and the minimal matching $M_-(Q,\underline{d}) = M_-$ via the procedures prescribed in Sections 3.2 and 3.3.1. Assign weights to the edges in M_- as prescribed in Definition 24. Note that we agree to associate the vector $\underline{e} = (0,0,\ldots,0)$, which trivially satisfies the all of Tran's conditions, to the minimal matching M_- which is in P by Proposition 34.

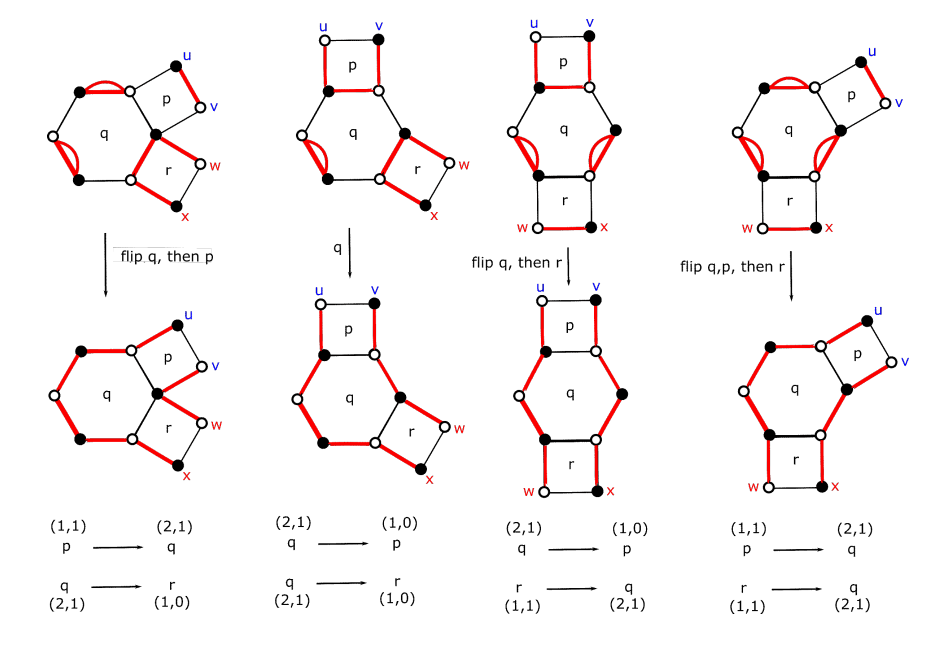
Suppose that we have some nonzero e satisfying all of Tran's conditions. To see that the resulting mixed dimer configuration D after our performing our algorithm is reachable by a sequence of allowable flips, we apply Lemmas 46 and 48. We proceed by induction on |e|. To establish the base case, we use M_{-} which is by definition reachable by an empty sequence of allowable flips. Suppose that up to $k \in \mathbb{N}$, our algorithm yields a mixed dimer configuration that is reachable by a sequence of allowable flips. Now suppose that |e| = k + 1 and that we have added 1 to the i^{th} entry of \underline{e} , i.e. flipped tile i. Note that as $i \to j$ is acceptable with respect to $(\underline{d}, \underline{e})$, we have that $e_i - e_j \leq \max(d_i - d_j, 0)$, i.e. $n_{i,j} \ge 0$. By Lemma 46, we have that $n_{i,j} = m_{i,j}$ which implies that the number of edges straddling tiles i and j must be non-negative. Moreover, by Lemma 48, since $0 \leq \underline{e} \leq \underline{d}$, we have that for any boundary edge α on tile i, $n_{i,\infty}(\alpha) = \max(d_i, 0) - e_i =$ $d_i - e_i \ge 0$ giving that $m_{i,\infty}(\alpha)$, the number of edges on α in D is non-negative. Similarly, $n_{\infty,i}(\alpha) = \max(-d_i, 0) + e_i = 0 + e_i \geqslant 0$ giving that $m_{\infty,i}(\alpha)$, the number of edges on α in D is non-negative. Hence, the resulting mixed dimer configuration D has edges with all non-negative weights. With this, we claim that there exists some reading of the entries of e (not simply left to right as the algorithm prescribes) which yields a mixed dimer configuration with non-negative weights at each flip along the way in the sequence.

Let j denote the label of a vertex of the quiver Q such that $e_j > 0$ and such that for any arrow pointing $i \to j$, we have $e_j > e_i$. Note that since |e| = k + 1 > 0 and Q is an oriented tree, it follows that such a vertex j exists. Consequently, if we let $\underline{e'}$ be the result of subtracting the j^{th} unit vector from \underline{e} , we see that (1) for every arrow $i \to j$, we have $n'_{i,j} = \max(d_i - d_j, 0) + (e_j - 1 - e_i)$ is nonnegative; (2) for every arrow $j \to i$, we have $n'_{j,i} = \max(d_j - d_i, 0) + (e_i - e_j + 1)$ is nonnegative; (3) the value $n'_{i,\infty} = d_i - e_i$ is nonnegative, and (4) the value $n'_{\infty,i} = e_i$ is nonnegative.

Hence, utilizing Lemmas 46 and 48, we see that e' corresponds to a mixed dimer configuration D'. Since |e'| = k, by the inductive hypothesis, D' is reachable by a sequence of allowable flips from M_- . Hence D itself is reachable from M_- by a sequence of allowable flips, where we tack on a flip of tile j. This last flip is allowable since both D' and D are mixed dimer configurations, i.e. with nonnegative weights on edges, and the difference $\underline{e} - \underline{e'}$ is the j^{th} unit vector.

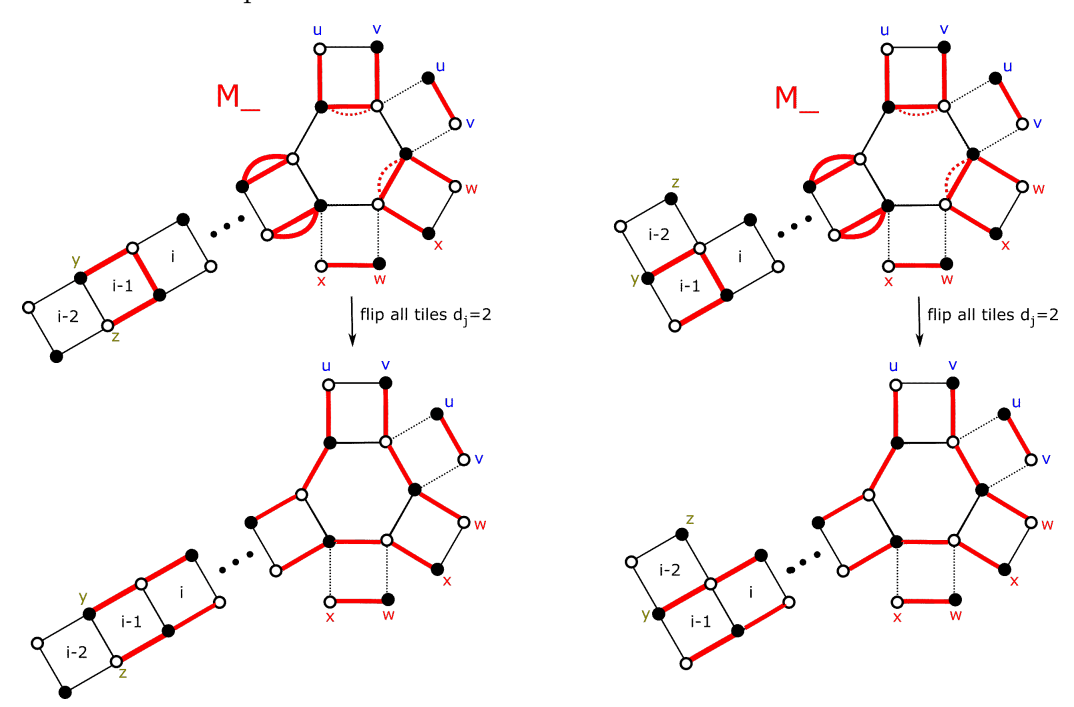
Hence, any mixed dimer configuration with non-negative weights must be reachable via a sequence of allowable flips from M_{-} . Therefore, since the resulting mixed dimer configuration D from our algorithm has all non-negative weights, it is reachable via a sequence of allowable flips from M_{-} .

The last thing we need to show is that the resulting mixed dimer configuration D is node-monochromatic. We again proceed by induction on |e|. By Proposition 34, we have that M_- is node-monochromatic, establishing the base case. So suppose that up to $k \in \mathbb{N}$, we have that when |e| = k, the resulting mixed dimer configuration D is node-monochromatic. Now take \underline{e} with |e| = k + 1 where we have added 1 to the i^{th} entry of \underline{e} . Since we have previously established that this mixed dimer configuration D is reachable by an allowable sequence of flips, we can assume that D was obtained via a sequence of k + 1 allowable flips from M_- . We claim that the only way we could have produced a path connecting nodes of different colors is if there is more than one critical arrow in Q with respect to $(\underline{d},\underline{e})$. We first show that if a path between $\underline{u},\underline{v}$ and $\underline{w},\underline{x}$ can be formed, then the corresponding quiver must have at least two critical arrows. We start with the minimal matchings for each orientation of the last three vertices n-3, n-2 and n-1 in Q and show that the only way to obtain paths between blue and red nodes via a sequence of allowable flips is when two critical arrows (namely, violating Tran's condition (3)) involving these three vertices arise:



By the symmetry of the vertices n-1 and n-2 in Q, it suffices to show no paths between green nodes to either blue or red can occur. To do this, we show that if such a path exists, there would be two critical arrows: one being the arrow $i \to i-1$ where d_i is the 2 in the \underline{d} -vector of maximal index and one involving the vertices n-3 and one of n-2 or n-1 (connecting to $\underline{u},\underline{v}$ or $\underline{w},\underline{x}$ respectively). To simplify the case work, suppose that one of the arrows $n-3 \to n-2$ and $n-3 \to n-1$ are critical. With this assumption, we can potentially make paths connecting both red to green and/or blue to green. We show that is this case, an additional critical arrow must be created in order to connect red or green to blue. Suppose that i is the 2 of maximal index in the \underline{d} vector. For the definition of where to place the nodes y, z, we need to examine the cases where i, i-1, i-2 are zigzagging or straight.

Note that if i-2 < 0, then this case reduces to the straight case. Suppose that the tiles i, i-1, i-2 are placed straight in G. Then, in order to create a path from either red or green to blue, we must flip all tiles with $d_j = 2$ for $j \ge i$ to obtain edges that are from white to black clockwise with respect to G_2 . This gives that $(d_j, e_j) = (2, 1)$ for all vertices $j \ge i$. When we flip tile i, note that we will connect the green nodes to both the red and blue nodes as pictured below in the left column:



We see that this must create a critical arrow $i \to i-1$ as $(d_i, e_i) = (2, 1)$ and $(d_{i-1}, e_{i-1}) = (1, 0)$. Now consider when i, i-1, i-2 are stacked in a zigzagging fashion in G. As before, in order to create a path from either red or green to blue, we must flip all tiles with $d_j = 2$ for $j \ge i$ to obtain edges that are from white to black clockwise with respect to G_2 . This gives that $(d_j, e_j) = (2, 1)$ for all vertices $j \ge i$. When we flip tile i, note that we will connect the green node j to the blue node j as pictured in the above figure on the right.

Thus, we see that via a sequence of allowable flips from M_- , this mixed dimer configuration will remain node-monochromatic as \underline{e} satisfies Tran's criticality condition. Hence, we have associated a mixed dimer configuration D in our poset P to our given vector \underline{e} satisfying all of Tran's conditions.

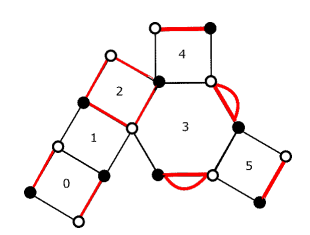
To continue our proof of Theorem 41, we now construct a map $D \longrightarrow \underline{e}$. The map sending $D \longrightarrow \underline{e}$ does not require the weighted version of flipping used in the previous theorem. For this direction of the bijection, we restrict our attention to allowable flips. This map is given by the superimposition of D with M_{-} and it is constructed via the following theorem:

Theorem 51. Given (Q,\underline{d},D) , there exists a unique way to produce \underline{e} that satisfies all of Tran's conditions i.e. conditions (1), (2), and (3) of Theorem 39. The process is given by the following procedure:

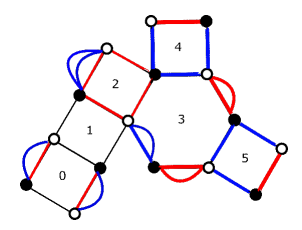
- 1. Let $\underline{v} = (0, 0, ..., 0) \in \mathbb{Z}^n$. Given (Q, \underline{d}, D) , construct the corresponding base graph and minimal matching M_- via the procedure described in Section 3.2.
- 2. Superimpose D with M_{-} to obtain the multigraph $M_{1} := D \sqcup M_{-}$.
- 3. Using the edges distinguished in D and M_- , create the largest cycle of length $\ell_1 > 2$, call it C_1 . (Note that C_1 may not be the unique cycle of length ℓ_1). For all faces i enclosed by C_1 , add +1 to v_i in \underline{v} and delete C_1 from M_1 . Call the resulting multigraph $M_2 = M_1 \setminus C_1$.
- 4. Examine M_2 and if there are any cycles of length $\ell_2 > 2$, find the cycle of largest length and call it C_2 . For all faces i enclosed by C_2 , add +1 to v_i and delete C_2 from M_2 .
- 5. Iterate this process of deleting cycles of of largest length and adding 1's to the vector \underline{v} until nothing is left besides 2-cycles. The resultant vector \underline{v} corresponds to \underline{e} .

Before proving this theorem, we compute an example:

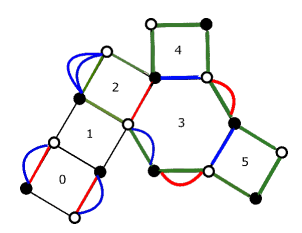
Example 52. Consider the quiver Q from Example 45 with the same positive root $\underline{d} = (1, 1, 2, 2, 1, 1)$. Suppose we start with the mixed dimer configuration $D \in P$ given by



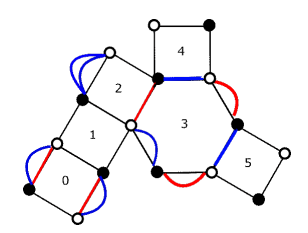
which is obtained by the sequence of allowable flips at tiles 3,2,4,5,3 in order. Superimposing this with the minimal matching, distinguished in blue, we obtain the multigraph as shown here.



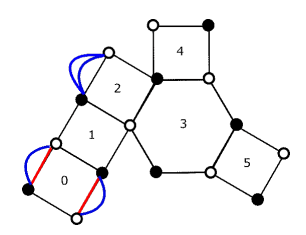
Following the algorithm stated in Theorem 51, we see the largest cycle we can create is of length 12 enclosing tiles 2,3,4 and 5, call it C_1 which we distinguish in green.



Deleting C_1 from our multigraph yields the resulting configuration as illustrated,



and since this cycle enclosed tiles 2,3,4 and 5, we now have that $\underline{v} = (0,0,1,1,1,1)$. Looking for the next largest cycle, we see that the cycle enclosing the hexagon i.e. tile 3 is largest, call it C_2 . Deleting C_2 from our multigraph, we obtain the figure below,



and we add +1 to v_3 , giving that $\underline{v} = (0, 0, 1, 2, 1, 1)$. Because there are only 2-cycles left in our multigraph, we have that $\underline{v} = (0, 0, 1, 2, 1, 1)$ is the \underline{e} we associate to D.

We now prove Theorem 51.

Proof. Let Q be a quiver of type D_n where the associated quiver is acyclic. Let $\underline{d} \in \Phi_+$. Obtain the base graph G(Q) = G and $M_-(Q,\underline{d}) = M_-$ via the procedure prescribed in Sections 3.2 and 3.3.1. Let $D \neq M_-$ be a mixed dimer configuration in P and initialize $\underline{v} = (0,0,\ldots,0)$.

We first illustrate why we can delete a cycle from the superimposition of D and M_- . Note that as both $D, M_- \in P$, they individually satisfy the valence condition. Hence, we obtain that each vertex that was previously valence 2 is now valence 4 in M_1 and each vertex that was valence 1 is now valence 2 in M_1 . Because $D \neq M_-$, there must exist some cycle of length at least 4 in their superimposition as D differs from the minimal matching by at least one allowable flip. Hence, there exists some cycle of maximal length $\ell_1 \geqslant 4$.

We aim to show that after each iteration of cycle deletion and adding the corresponding 1's to the entries in the vector \underline{v} , the resultant vector satisfies all of Tran's conditions.

Tran Condition (1). We claim that Condition (1) of Theorem 39, i.e. $0 \le \underline{v} \le \underline{d}$ is satisfied. Note that the only way a cycle can enclose tile j in the superimposition of D and M_{-} is if D differs from M_{-} at a tile j. The only way this could happen is if an allowable flip occurred at tile j. By definition of allowable flip, we require that $d_j > 0$. Moreover, the only positive entries in \underline{v} correspond to tiles enclosed by some cycle C_i in our algorithm. The only way $v_j > d_j$ is if $v_j = 2$ and $d_j = 1$. However, this would imply that the tile j was enclosed by two cycles in our algorithm i.e. the tile j can be flipped twice. This can only happen in $d_j = 2$. Hence, $v_j \le d_j$ for all j giving that $0 \le \underline{v} \le \underline{d}$.

Tran Condition (2). In order to prove the other two Tran conditions, we will be using two forms of induction. We will be inducting of the number of iterations needed such that nothing is left in $D \sqcup M_-$ but a disjoint union of 2-cycles. Within this induction, we will also induct on the number of tiles that each cycle in the algorithm encloses. We can establish the base case of both inductions immediately as we agree to associate M_- to $\underline{e} = (0, 0, \ldots, 0)$ which trivially satisfies Tran's conditions (2). We first claim that deleting C_i and adding the appropriate 1's to \underline{v}' , we obtain a vector \underline{v} that satisfies Tran's acceptability condition, i.e. Condition (2) of Theorem 39. In order to do this, we now induct on the number of tiles enclosed by C_i .

Suppose that C_i encloses one face, call it j. In order to check that \underline{v} is acceptable in this case, it suffices to check that any arrows involving vertex j satisfies the acceptability condition. Note that $v_j = 1$ or 2 because j could have been enclosed in a previous cycle in an earlier iteration. We first address the case when $v_j = 1$. Also, suppose that j is the tail of an arrow $k \to j$. In this case, when $v_k \neq 2$, the acceptability is trivially satisfied as $v_k - v_j \leq 0$. So, we consider when $v_k = 2$ which gives us that $v_k - v_j = 1$. Note that all the cases where acceptability fails, i.e. when $\max(d_k - d_j, 0) = 0$, are precisely the cases where

$$n_{k,j} = \max(d_k - d_j, 0) + (v_j - v_k) = 0 - 1 = -1.$$

However, this violates Corollary 47 which tells us that all edges weights must be nonnegative. Hence, these cases are impossible.

Now suppose that j is the head of an arrow, i.e. $j \to k$ in Q. In this case, when $v_k \neq 0$, the acceptability is trivially satisfied as $v_k - v_j \leq 0$. So, we consider when $v_k = 0$

which gives us that $v_j - v_k = 1$. Note that all the cases where acceptability fails, i.e. when $\max(d_j - d_k, 0) = 0$, are precisely the cases where

$$n_{i,k} = \max(d_i - d_k, 0) + (v_k - v_i) = 0 - 1 = -1.$$

Again, this violates Corollary 47 as all edge weights must be nonnegative. Hence, this cases is also impossible.

Now suppose that $v_j = 2$. Note that j is the tail of an arrow $k \to j$, the acceptability is trivially satisfied as $v_k - v_j \le 0$ for any choice of v_k . So, it suffices to consider when j is the head of an arrow, i.e. $j \to k$ in Q. In this case, when $v_k = 2$, the acceptability is trivially satisfied as $v_j - v_k = 0$. So, we consider when $v_k = 0$ or 1. If $v_k = 1$, then $v_j - v_k = 1$ and all the cases where acceptability fails, i.e. when $\max(d_j - d_k, 0) = 0$, are precisely the cases where

$$n_{j,k} = \max(d_j - d_k, 0) + (v_k - v_j) = 0 - 1 = -1.$$

However, this again violates Corollary 47. Similarly, if $v_k = 0$, then $v_j - v_k = 2$. Then, all the cases where acceptability fails, i.e. when $\max(d_k - d_j, 0) \leq 1$, are precisely the cases where

$$n_{j,k} = \max(d_j - d_k, 0) + (v_k - v_j) < 0$$

violating Corollary 47. Hence, these cases are impossible. Therefore, we have established the base case for our induction on the number of tiles enclosed by C_i .

Now, assume that if C_i enclosed k tiles, then \underline{v} satisfies Tran's acceptability condition. Now, suppose that C_i encloses k+1 tiles, t_1, \ldots, t_{k+1} . We aim to show that $\underline{v} + \underline{e_{t_{k+1}}} = \underline{y}$ satisfies Tran's acceptability condition.

Again, by our inductive hypothesis, it suffices to show that any arrow with vertex t_{k+1} still satisfies the acceptability condition. Since tile t_{k+1} is enclosed by C_i and may have been enclosed by another cycle in a previous iteration, we have that $y_{t_{k+1}} \geq 1$. If j is the other vertex in an arrow involving t_{k+1} , we also have to consider all possible values of $d_j, y_j, d_{t_{k+1}}$ as well as if t_{k+1} is the head or tail of the arrow. First, suppose that $y_{t_{k+1}} = 1$ which means that $d_{t_{k+1}} = 1$ or 2. Next, suppose that t_{k+1} is the tail of an arrow, i.e. $j \to t_{k+1}$ in Q. When $y_j < 2$, the acceptability condition is trivially satisfied as $y_j - y_{t_{k+1}} \leq 0$. So suppose that $y_j = 2$ and since $y_j \leq d_j$, this implies that $d_j = 2$. As $d_j \geq 1$, the acceptability condition is satisfied in all cases.

Now, still suppose that $y_{t_{k+1}} = 1$, but now suppose that t_{k+1} is the head of an arrow, i.e. $t_{k+1} \to j$ in Q. When $y_j > 0$, the acceptability condition is trivially satisfied as $y_{t_{k+1}} - y_j \leq 0$. So suppose that $y_j = 0$, note that if $d_{t_{k+1}} - d_j \geq 1$, the acceptability condition is satisfied. When $d_{t_{k+1}} - d_j \leq 0$, this means that

$$n_{t_{k+1},j} = \max(d_{t_{k+1}} - d_j, 0) + (y_j - y_{t_{k+1}}) = -1$$

violating Corollary 47. Hence, these cases are impossible. Now, suppose that $y_{t_{k+1}} = 2$ which means that $d_{t_{k+1}} = 2$. Note that when t_{k+1} is the tail of an arrow, i.e. $j \to t_{k+1}$ in Q, $y_j - y_{t_{k+1}} \leq 0$ giving that acceptability is trivially satisfied. So suppose that t_{k+1} is the head of an arrow, i.e. $t_{k+1} \to j$ in Q. When $y_j = 2$, the acceptability condition is trivially satisfied as $y_{t_{k+1}} - y_j = 0$. So suppose that $y_j = 1$ or 2, note that as $d_{t_{k+1}} = 2$, the acceptability condition only fails if $y_j < d_j$. But this is precisely when

$$n_{t_{k+1},j} = \max(d_{t_{k+1}} - d_j, 0) + (y_j - y_{t_{k+1}}) = -1$$

violating Corollary 47. Hence, these cases are impossible. Therefore, we have shown that if C_i encloses k+1 cycles, the resulting vector \underline{y} satisfies Tran's acceptability condition. By induction, we have that after the i^{th} step of our algorithm, \underline{v} satisfies Tran's acceptability condition. Therefore, any vector obtained via this algorithm must satisfy the acceptability condition. Hence, the resultant \underline{e} must be acceptable.

Tran Condition (3). We now show that the criticality condition, Tran's condition (3), is satisfied by \underline{v} . In order to do this, we again induct on the number of steps needed to complete our algorithm. Furthermore, we induct on the number of tiles enclosed by C_i at each step.

To establish the base cases of both inductions, suppose that C_1 encloses a unique tile j. Then $\underline{v} = \underline{e_j}$, the unit vector with a 1 in the j^{th} position. Note that if $d_j \neq 2$, no critical arrows can be formed as $S := \{i \in Q : (d_i, e_i) = (2, 1)\} = \emptyset$. So, suppose that $d_j = 2$. Then, as $(d_j, v_j) = (2, 1)$, $j \in S$ and the only way that the criticality condition could have failed is if this created two critical arrows i.e.

$$k \longleftarrow j \longrightarrow \ell$$

(1,0) \leftarrow (2,1) \rightarrow (1,0)

where we must have $v_k = 0 = v_\ell$ as the only tile enclosed by a cycle is j. Note that since the subgraph G_2 associated to all tiles with d entry 2 is connected, this means that j must be the unique tile in G_2 . By the structure of the positive root $\underline{d} \in \Phi_+$, we have that j must be on the tile associated to the hexagon, i.e. vertex n-3 in Q. Hence, our base graph is:

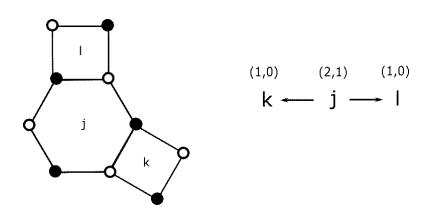


Figure 2

based on the orientation of the quiver. In this case, our minimal matching and mixed dimer configuration D will locally look like the following:

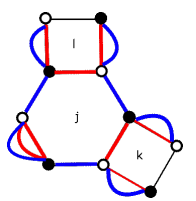


Figure 3

where we obtained the minimal matching, distinguished in red, with the convention that we distinguish edges going black to white in the bipartite coloring and obtain D, distinguished in blue, by performing an allowable flip at tile j. We now have two cases: either both k, ℓ are terminal vertices, i.e. are degree one in the quiver, or one of k or ℓ is terminal and the other is not, meaning it has degree two in the quiver. Suppose that both k, ℓ are terminal. With the labeling of the nodes as prescribed in Section 3.4.1, we see that the mixed dimer configuration D has two paths connecting nodes of different colors.

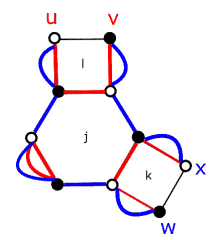


Figure 4

This means that $D \notin P$ which is a contradiction. Now, without loss of generality, suppose that k is the terminal vertex and ℓ has degree two in the quiver. Since j is the minimal index with $d_j = 2$ in \underline{d} , the nodes y, z will either be placed on tile $\ell = j - 1$ or j - 2 depending on the orientation of the arrows connecting $j, \ell, j - 2$. In either case, we see paths between nodes of different colors formed:

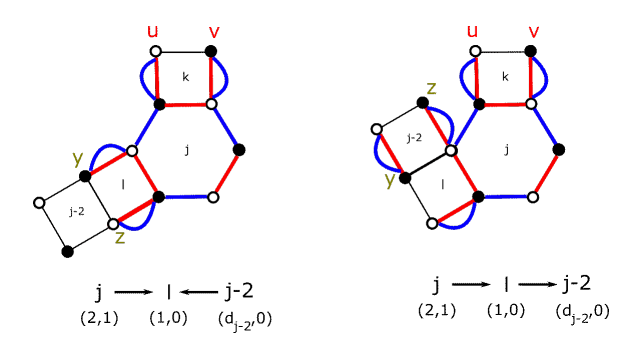


Figure 5

Hence, two critical arrows cannot be formed if C_1 encloses a single tile. Now, suppose that if C_1 encloses k tiles, the resulting vector \underline{v} satisfies the criticality condition. We now aim to show that if C_1 encloses k+1 tiles, then the resulting vector $\underline{w} := \underline{v} + e_j$ satisfies

the criticality condition. Note that by our inductive assumption, $(\underline{v},\underline{d})$ has at most one critical arrow. Suppose that $(\underline{v},\underline{d})$ created 0 critical arrows. Since \underline{w} only differs from \underline{v} in the j^{th} entry, it suffices to only check any arrows involving j. Moreover, we need to show that two critical arrows cannot be created by adding +1 to the j^{th} entry of \underline{v} to obtain \underline{w} . The only way that this could happen is if j is the unique vertex in S, i.e. d_j is the unique 2 in \underline{d} with a quiver of one of the following orientations:

$$p \leftarrow j \leftarrow q$$
 (i)

$$(1,0) \leftarrow (2,1) \leftarrow (1,1)$$

$$p \longrightarrow j \longrightarrow q$$
 (ii)

$$(1,1) \to (2,1) \to (1,0)$$

$$p \leftarrow j \rightarrow q$$
 (iii)

$$(1,0) \leftarrow (2,1) \rightarrow (1,0)$$

$$p \longrightarrow j \longleftarrow q$$

$$(1,1) \to (2,1) \leftarrow (1,1)$$
(iv)

Note that case (iv) will not be possible as if $w_p = w_q = 1$. This means that both p and q were enclosed by C_1 . However, since j is in between these vertices, this impossible without having enclosed j as well by the connectedness of the tiles enclosed by C_1 .

Note that we analyzed case (iii) in the base case. Namely, since C_1 enclosed a connected set of tiles, we must have that p, q are terminal which puts us in the case of Figure 4.

Also note that cases (i), (ii) are symmetric. So it suffices to focus on case (i). Based on the orientations of the arrows, our base graph is up to isometry/ bipartite coloring is one of the following:

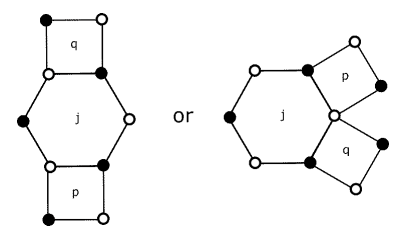


Figure 6

Within these cases, we have to consider if p, q are terminal vertices in the quiver. This gives that for each of these base graphs, there are two cases: either both p, q are terminal in Q or one of p or q is terminal in Q. Suppose that the base graph is given by the left graph in Figure 6. Then, if both p, q are terminal, we obtain the mixed dimer configuration D by performing allowable flips at tile j, then tile q. In this case, we see D is node-polychromatic as:

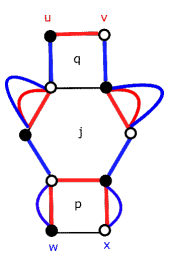


Figure 7

Without loss of generality, suppose that q is terminal and p has degree 2 in Q. Namely, in either case of the orientation of this arrow, we see D is node-polychromatic as:

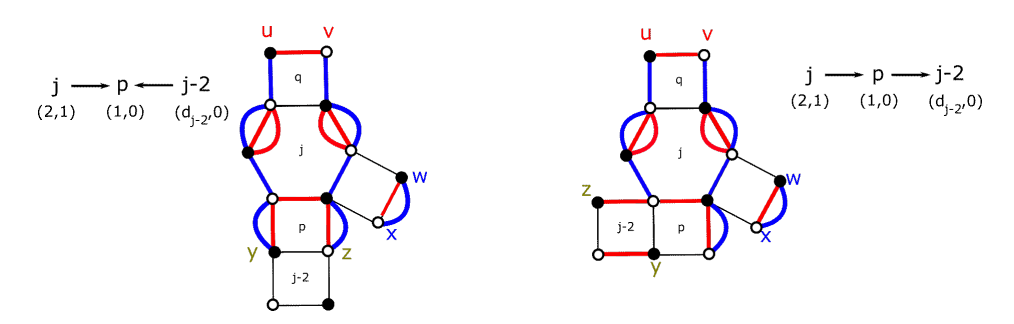


Figure 8

Now, suppose the base graph is given by the right graph in Figure 6 and suppose that both p, q are terminal. Then, we see D is node-polychromatic as:

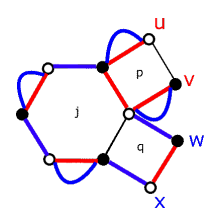


Figure 9

Without loss of generality, suppose that q is terminal and p has degree 2 in Q. Namely, in either case of the orientation of this arrow, we analyzed isometric copies of these cases in Figure 8 and saw they produce node-polychromatic mixed dimer configurations.

So, if no critical arrows were created when C_1 enclosed k tiles, we have shown that two critical arrows are not created when C_1 encloses k+1 tiles. Now suppose that one critical arrow is created if C_1 encloses k tiles. We now aim to show that enclosing k+1 tiles creates no critical arrows. Note that $S \neq \emptyset$ as one critical arrow was created. Suppose that $s \in S$, i.e. $(d_s, w_s) = (2, 1)$, and as $v_s = 1$, we know that s must have been enclosed by C_1 . Note that if j were not connected to s, then the only way another critical arrow

can be made is if $(d_j, v_j) = (2, 1)$. However, entries that are 2 in $\underline{d} \in \Phi_+$ are consecutive, so this cannot happen. So suppose that j is connected to s. The only way that another critical arrow can be made is if either $j \to s$ with $(d_j, w_j) = (1, 1)$ and $(d_s, w_s) = (2, 1)$ or $j \leftarrow s$ with $(d_j, w_j) = (1, 0)$ and $(d_s, w_s) = (2, 1)$. However, note that the ladder case is impossible as $w_j = 1$ by hypothesis that j is enclosed by C_1 . This gives that we are in one of the following two situations:

$$j \longrightarrow s \longleftarrow t \tag{a}$$

$$(1,1) \to (2,1) \leftarrow (1,1)$$

$$j \leftarrow s \longrightarrow t$$

$$(1,0) \leftarrow (2,1) \rightarrow (1,0).$$
(b)

Note that case (b) was done previously where j plays the role of q and s plays the role of j in case (i) where we assumed that zero critical arrows were formed with C_1 enclosing k tiles. So, we only need to address case (a). Again, $s \in S$ must be the unique vertex with $d_s = 2$ as the 2's are consecutive in any positive root which gives us that s must be the hexagon. Note that with the orientation of the arrows, the only possibility for the base graph up to isometry is:

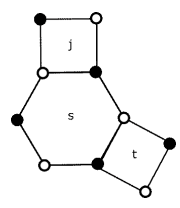


Figure 10

Now we consider if j, t are terminal vertices. If j, t are both terminal, note that a node-polychromatic mixed dimer configuration is produced as:

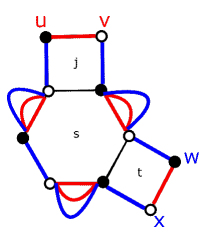


Figure 11

Without loss of generality, suppose that j is terminal and t has degree 2 in Q. Then, we need to consider the other arrow with vertex t to use the nodes y, z. In these cases, we obtain paths between nodes of different colors:

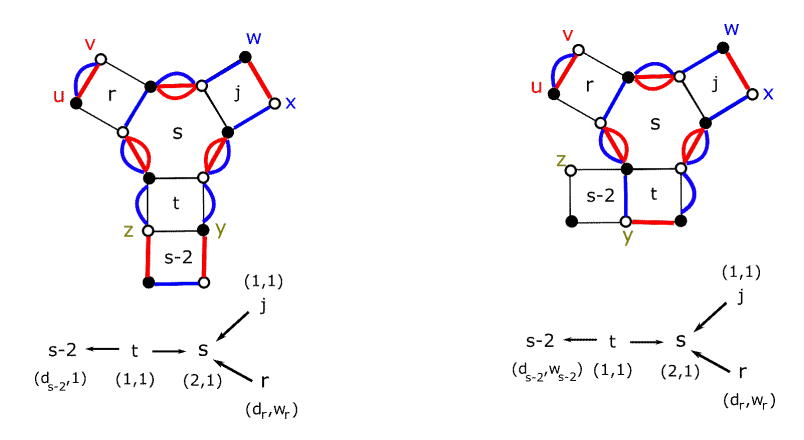


Figure 12

Note that in both figures, it does not matter what (d_r, w_r) are because even if $w_r > 0$, this does not affect the path formed between x and y. In fact, it creates another path connecting nodes of different colors from u to z. Therefore, we have shown that if one critical arrow was formed by enclosing k tiles, then no critical arrows are created when enclosing k+1 tiles. Hence, by induction, we have proven that if C_1 encloses n tiles, then \underline{v} satisfies the criticality condition which establishes the base case of our induction on the number of steps of our algorithm.

Suppose that up the i^{th} step of our algorithm, each \underline{v} satisfies the criticality condition. We now aim to show that after removing C_{i+1} to create \underline{v} , we still satisfy the criticality condition. To do this, we again induct on the number of tiles enclosed by cycle C_{i+1} . Suppose that C_{i+1} enclosed a single tile j. Note that we cannot create any additional critical arrows if j was enclosed in a previous cycle as $v_j = 2$, so we suppose that $v_j = 1$. Again, either 0 or 1 critical arrows were created with $(\underline{v},\underline{d})$. In either case, this reduces to the argument made in the base case for C_1 with the only difference being that $v_m = 2$ for some vertices m. But note that this will not affect the analysis of creating critical arrows because the definition of critical arrows require that $v_m = 0, 1$.

Suppose that C_{i+1} encloses k tiles and that the associated vector satisfies the criticality condition. Now, we aim to show that if C_{i+1} encloses k+1 tiles, then the resulting vector \underline{w} still satisfies the criticality condition. As in the base case above, note that we cannot create any additional critical arrows if j was enclosed in a previous cycle as $v_j = 2$, so we suppose that $v_j = 1$. Similarly, note that even if some $v_m = 2$, this will not affect the analysis of creating critical arrows because the definition of critical arrows require that $v_m = 0, 1$. So, this case reduces to the base case of the inductive step even if $w_{j-2} > 0$.

So, we see that by definition of the mixed dimer configuration D being node- monochromatic that the criticality condition is satisfied by \underline{v} . By induction, enclosing m tiles with C_{i+1} results in \underline{v} that satisfies Tran's condition (3). This gives that after each step of our algorithm, the resulting vector \underline{v} must satisfy Tran's condition (3). Therefore, the resulting vector \underline{e} must satisfy all of Tran's conditions.

We now show that these maps described in Theorems 44 and 51 are indeed inverses of one another. For an example of this, see that Examples 45 and 52 are inverses of each other. This completes the proof of Theorem 41.

Proof. In order to show that these maps are inverses of each other, first note that by definition of the algorithm in Theorem 44, we see that the number of steps in the algorithm exactly equals |e|, where \underline{e} is the resulting vector associated to D. Therefore, it makes sense to induct on |e|.

For the base case, suppose that |e| = 0, i.e. we do not perform any steps of the algorithm in Theorem 44. Then, by conventions of both algorithms for Theorems 51 and 44, we have that e is associated to M_{-} and vice versa.

Suppose up to $k \in \mathbb{N}$, when |e| = k, i.e. we perform k steps of our algorithm in Theorem 44, these maps are inverses of one another. Let \underline{e} such that |e| = k + 1 where we added 1 to the i^{th} entry of \underline{e}' where |e'| = |e| - 1 = k. Suppose that by Theorem 44, we associated the mixed dimer configuration D' corresponding to \underline{e}' and D is the mixed dimer configuration associated to \underline{e} . Note that as |e| = k + 1, we had to perform k + 1 flips from M_- to obtain D and by assumption, we had to perform one more flip at tile i to obtain D from D'.

We aim the show that using the algorithm in Theorem 51, we have that our initial vector \underline{e} is the vector associated to D. If we take the superimposition of $D \sqcup D'$, note that will consist of all 2-cycles and exactly one 4-cycle enclosing tile i. This implies that $D \sqcup M_-$ will also have at least one cycle containing i. Moreover, $D \sqcup M_-$ will have exactly one more cycle containing i that that of $D' \sqcup M_-$. Hence, the corresponding vector obtained by performing the algorithm in Theorem 51 must be $\underline{e}' + e_i$ which is exactly \underline{e} .

Now suppose that given a mixed dimer configuration D, using the algorithm in Theorem 51, we obtain an \underline{e} such that |e| = k + 1. Let D' be the mixed dimer configuration associated to $\underline{e'} = \underline{e} - \underline{e_i}$, i.e. subtracting 1 from the i^{th} entry of \underline{e} . By the prescription of the algorithm in Theorem 51, we must have enclosed the tile i e_i number of times when looking at D and $(e_i - 1)$ number of times when looking at D'. By our inductive assumption, let $\underline{e'}$ be associated to D'. Note that the order in which we flip tiles in the algorithm in Theorem 44 does not matter, so to obtain the mixed dimer configuration D from D', it suffices to flip the tile i. Therefore, we see that the mixed dimer configuration associated to \underline{e} prescribed by the algorithm in Theorem 44 is exactly the mixed dimer configuration D we began with.

Therefore, we see that these maps are indeed inverses of each other. Thus, our graphical model bijects to that of Tran's. \Box

4.2.2 Coefficients

To show that our model gives the exact F-polynomial associated to $\underline{d} \in \Phi_+$, all that is left to do is show that our model gives the right coefficients, i.e. show that the coefficient of $u_0^{e_0} \cdots u_{n-1}^{e_{n-1}}$ is 2^c , where c is the number of cycles in the mixed dimer configuration associated to \underline{e} . Note that when we refer to cycles, we insist the length of the cycle is larger than 2. To show our model yields the correct coefficients, we show that the number of cycles in D corresponds to the number of connected components C of S with $\nu(C) = 0$.

First note that we cannot have a cycle on a tile that is a dimer configuration, i.e. we need $d_i = 2$ in order for i to potentially be enclosed by a cycle. Also, note that there are no cycles in M_- by the convention of the black and white coloring in the definition of M_- , so in order for tile i to be enclosed by a cycle, we must have that $e_i \ge 1$. This tells us that the set of all tiles that can potentially be enclosed by a cycle are contained within $S = \{i \in Q : (d_i, e_i) = (2, 1)\}.$

Fix D associated to $(\underline{d},\underline{e})$. Let C be a connected component of S. Suppose that $\nu(C) \neq 0$, that is, there is some $c \in C$ such that c is the vertex of a critical arrow. Namely, this c must be connected to a tile outside of S by definition of the d, e coordinates of the other vertex of the critical arrow. Let c' be the other vertex of the critical arrow involving c. Note that if $c \to c'$ about the edge α , then $(d_{c'}, e_{c'}) = (1, 0)$ and we have that $n_{c,c'} = \max(d_c - d_{c'}, 0) + (e_{c'} - e_c) = 1 - 1 = 0$. If $c' \to c$ about the edge α , then $(d_{c'}, e_{c'}) = (1, 1)$ and we have that $n_{c',c} = \max(d'_c - d_c, 0) + (e_c - e_{c'}) = 0$. Therefore, by Lemma 46, the edge α cannot have an edge from D which tells us that no cycle in D can enclose tile c. This tells us that if a cycle encloses any tile or collection of tiles in C, then $\nu(C) = 0$.

Now, suppose that C is a connected component of S with $\nu(C) = 0$, i.e. no critical arrows involve any vertex c from C. Suppose that C is comprised of the tiles i, \ldots, m where i is the minimal tile in C and m is the maximal tile in C with respect to the indexing in Q. We aim to show that there exists a cycle in D enclosing all of C. Note that for $i \leq j \leq m-1$, we have that $(d_j, e_j) = (2, 1)$, so there are no edges in D on the edge straddling tiles j and j+1 by Lemma 46 since $n_{j,j+1} = 0$. This implies that if we can show that all the boundary edges of C are in D, that there is a cycle enclosing all of C in D.

Note that as $e_j = 1$ for all $i \leq j \leq m$, we have that each of the tiles in C have been flipped exactly once from M_- using our bijection of adding 1's to the \underline{e} -vector coinciding with flipping the corresponding tile from Theorem 51. Note that if a boundary edge α on tile t is oriented black to white clockwise with respect to G_2 , then by definition of M_- , α must have two edges distinguished in M_- . After one flip at tile t, $w(\alpha)$ decreases by 1. This gives that this edge now has exactly one edge in D. On the other hand, if α is oriented white to black clockwise with respect to G_2 , then by definition of M_- , α has no

edges distinguished in M_- . After performing a flip on tile t, we have that $w(\alpha)$ increases by 1. This gives that α now has exactly one edge distinguished in D. Hence, all the edges of the cycle enclosing C that are on the boundary of G have exactly one edge on them in D.

Now, we need to show that the cycle closes up on the interior edges of G, i.e. if i > 0 and/or m < n - 1, we need to verify that the edges straddling tiles i, i - 1 and m, m + 1 have one edge distinguished in D. Note that as $i, m \in C$ with $\nu(C) = 0$, no arrow involving i or m is critical. By structure of $\underline{d} \in \Phi_+$, we have that $d_{i-1} \ge 1$ and $d_{m+1} \ge 1$. Seeking a contradiction, suppose that $n_{i,i-1} = 0$. Then, $\max(d_i - d_{i-1}, 0) = e_i - e_{i-1}$, i.e. $\max(2 - d_{i-1}, 0) = 1 - e_{i-1}$. Since $e_{i-1}, d_{i-1} \in \{0, 1, 2\}$, this only occurs if either $d_{i-1} = 1$ giving that $e_{i-1} = 0$ or if $d_{i-1} = 2$ giving that $e_{i-1} = 1$. In the first case, this gives that the arrow $i \to i - 1$ is critical which contradicts that $\nu(C) = 0$. In the second case, $i - 1 \in C$ which contradicts the minimality of i. Hence, $n_{i,i-1} > 0$ and by Lemma 51, this means there must be an edge straddling tiles i, i - 1 in i. Note that this same argument holds for showing that there must be an edge in i straddling tiles i, i - 1 in i. Therefore, we see that one cycle is formed around all of i when i so i with i the number of cycles in i is exactly the number of connected components i of i with i or i therefore, the coefficients from our graphical model match those in Tran's.

Example 53. Note that in Examples 45 and 52, the mixed dimer configuration D has a cycle enclosing the tile 2. From Example 36, we see the term in the F-polynomial associated to this dimer configuration D has the coefficient of 2^1 .

4.3 Direct Connection to Quiver Grassmannian

Now that we have shown the connection between our model and that of Thao Tran, we can state the direct connection between our model and the quiver Grassmannian.

Corollary 54. Let Q be an acyclic quiver of type D_n and \underline{d} be a positive root in the root system. Let M be the corresponding indecomposable representation of Q of dimension \underline{d} . Then

$$\sum_{D \in P} 2^{\#\{cycles\ in\ D\}} y(D) = \sum_{\substack{\underline{e} \in \mathbb{Z}^n \ such\ that \\ 0 \le e_i \le d_i}} \chi_{\underline{e}}(M) y_1^{e_1} \cdots y_n^{e_n}$$

where $\chi_{\underline{e}}(M)$ is the Euler Poincaré characteristic of the Quiver Grassmannian $Gr_{\underline{e}}(M)$.

Loosely speaking, an acceptable flip at tile i corresponds to increasing the dimension of the vector space at vertex $i \in Q$ in a subrepresentation N of M. Moreover, our notion of node-connectivity corresponds to avoiding conflicts in choices of 1-dimensional subspaces of 2-dimensional vector spaces. Paths between nodes of different colors indicate inconsistent choices of subspaces on the vertices in N.

5 Computation of g-vectors from our model

Since we have established that our dimer configuration model gives a graph-theoretic interpretation of the F-polynomial, it is natural to want an interpretation of the g-vector from our model. By [FZ07], the data of F-polynomials and g-vectors is equivalent to the data of Laurent expansions of cluster variables. In particular, this data is in a sense richer because it yields the Laurent expansions of the cluster variables decorated with principal coefficients.

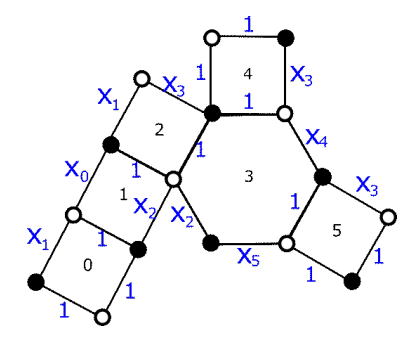
To give the interpretation of the g-vector, we must establish an edge weighting on the minimal matching M_- associated to some acyclic quiver Q of type D_n and a positive root $\underline{d} \in \Phi_+$. Note that this is a separate notion from the definition of "weighted flip" given in Section 42. Following the edge weights of [MS10], we define the edge weights of the base graph associated to Q as follows:

- 1. For any internal edge e, define wt(e) = 1.
- 2. For any arrow $j \to i$, on tile j, weight a white to black clockwise with respect to j boundary edge by x_i . On tile i, weight a black to white clockwise with respect to i boundary edge by x_j .
- 3. Otherwise, weight the edge 1.

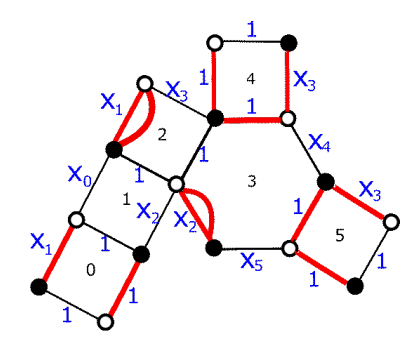
Remark 55. In step 2 of the definition of the edge weights from above, there is an ambiguity. Namely if there are multiple black to white clockwise with respect to tile j boundary edges α, β of j, we can choose either α or β to assign weight of x_i . It turns out that this choice does not affect the edge-weighting of matchings given the proof of Theorem 57 below.

Define the weight of the minimal matching $M_{-}=M_{-}(Q,\underline{d})$, denoted wt (M_{-}) , to be the product of the edge weights distinguished in M_{-} . Let's see this definition in the following example:

Example 56. Let Q be the D_6 quiver in Example 45. Then, we assign the following weights to the edges of the base graph:



If we consider the positive root $\underline{d} = (1, 1, 2, 2, 1, 1)$, then we obtain the following minimal matching which has $\operatorname{wt}(M_{-}) = x_1^3 x_2^2 x_3^2$.



With this choice of weighting, we have the following result:

Theorem 57. The g-vector associated to Q and a positive root $\underline{d} \in \Phi_+$, denoted $\underline{g} = g(Q,\underline{d})$, is given by

$$\underline{g} = \deg\left(\frac{wt(M_{-})}{\underline{x}^{\underline{d}}}\right)$$

where $deg(x_0^{a_0}x_1^{a_1}\cdots x_{n-1}^{a_{n-1}}) := (a_0, a_1, \dots, a_{n-1}).$

Before proving this result, we return to Example 56.

Example 58. Through direct computation, the associated g-vector is given by (-1, 2, 0, 0, -1, -1) and using Theorem 57, we see that

$$\deg\left(\frac{\operatorname{wt}(M_{-})}{\underline{x}^{\underline{d}}}\right) = \deg\left(\frac{x_1^3 x_2^2 x_3^2}{x_0 x_1 x_2^2 x_3^2 x_4 x_5}\right) = \deg(x_0^{-1} x_1^2 x_2^0 x_3^0 x_4^{-1} x_5^{-1}) = (-1, 2, 0, 0, -1, -1).$$

Proof. Theorem 4.4 in [Tra09] gives an interpretation of the g-vector in terms of the data $(\underline{e},\underline{d})$ where \underline{e} is a vector that again satisfies conditions (1)-(3) in Theorem 39. Namely it says that given a classical type acyclic quiver Q, the \underline{g} -vector $\underline{g}_{\underline{d}}$ corresponding to $\underline{d} \in \Phi_+$ is

$$-\sum_{i=1}^{n} d_i \underline{e_i} + \sum_{i,j=1}^{n} d_i \max(-b_{ji}, 0) \underline{e_j}$$

where b_{ji} denotes the $(j,i)^{\text{th}}$ entry of the exchange matrix associated to the quiver Q. Note that we can re-express this statement for the \underline{g} -vector in terms of the quiver Q and the positive root $\underline{d} \in \Phi_+$:

$$\underline{g} = \deg \left(\frac{\prod_{i \in Q_0} \prod_{j \to i} x_j^{d_i}}{\underline{x}^{\underline{d}}} \right).$$

This is because the denominator of the above expression coincides with Tran's term $-\sum_{i=1}^{n} d_i e_i$ and since we weight the black to white clockwise orientation with x_i with

 $j \to i$ which coincides with Tran's term $\sum_{i,j=1}^{n} d_i \max(-b_{ji}, 0) \underline{e_j}$. Hence, we can reexpress Tran's Theorem 4.4 in this way. Moreover, by definition of M_- , this expression is the same as

$$\underline{g} = \deg\left(\frac{\operatorname{wt}(M_{-})}{\underline{x}^{\underline{d}}}\right). \quad \Box$$

Corollary 59. Theorem 35 and Theorem 57 give the full Laurent expansions of cluster variables. Namely, for an acyclic quiver Q of type D_n , and positive root $\underline{d} \in \Phi_+$, we have that

$$x_{Q,\underline{d}} = F_{\underline{d}}(\hat{y_0}, \hat{y_1}, \dots, \hat{y_{n-1}}) x_0^{g_0} x_1^{g_1} \cdots x_{n-1}^{g_{n-1}},$$

where $\hat{y_i} = y_i \prod_{j=0}^{n-1} x_j^{-b_{ji}^0}$.

To see what the Laurent expansions for the cluster variables are, let's look at an example.

Example 60. Let $\underline{d} = (1, 1, 2, 1, 1) \in \Phi_+$ and let Q be the following orientation of D_5 .

$$0 \leftarrow 1 \leftarrow 2 \stackrel{\checkmark}{\searrow}_{4}^{3}$$

Then our F-polynomial is given by

$$F_{\underline{d}} = 1 + u_0 + u_4 + u_0 u_1 + u_0 u_4 + u_2 u_4 + u_0 u_1 u_4 + u_0 u_1 u_2 + u_0 u_2 u_4 + 2u_0 u_1 u_2 u_4 + u_0 u_1 u_2 u_3 u_4 + u_0 u_1 u_2^2 u_4 + u_0 u_1 u_2^2 u_3 u_4,$$

and our g-vector is $\underline{g} = (-1, 0, 0, -1, -1)$. In order to get our cluster variables, we evaluate the F-polynomial at \hat{y}_i and then multiply by $x^{\underline{g}}$. Note that

$$\hat{y_0} = y_0 x_1^{-1}$$
 , $\hat{y_1} = y_1 x_0 x_2^{-1}$, $\hat{y_2} = y_2 x_1 x_3^{-1} x_4$, $\hat{y_3} = y_3 x_2$, $\hat{y_4} = y_4 x_2^{-1}$.

This gives that the F-polynomial is

$$\begin{split} F_{\underline{d}}(\hat{y_0}, \hat{y_1}, \hat{y_2}, \hat{y_3}, \hat{y_4}) &= 1 + y_0 x_1^{-1} + y_4 x_2^{-1} + \frac{y_0 y_1 x_0}{x_1 x_2} + \frac{y_0 y_4}{x_1 x_2} + \frac{y_2 y_4 x_1 x_4}{x_2 x_3} + \frac{y_0 y_1 y_4 x_0}{x_1 x_2^2} \\ &\quad + \frac{y_0 y_1 y_2 x_0 x_4}{x_3} + \frac{y_0 y_2 y_4 x_4}{x_2} + \frac{2y_0 y_1 y_2 y_4 x_0 x_4}{x_2^2 x_3} + \frac{y_0 y_1 y_2 y_3 y_4 x_0 x_4}{x_2 x_3} \\ &\quad + \frac{y_0 y_1 y_2^2 y_4 x_0 x_1 x_4^2}{x_2^2 x_3^2} + \frac{y_0 y_1 y_2^2 y_3 y_4 x_0 x_1 x_4^2}{x_2 x_3^2}. \end{split}$$

Therefore, the cluster variable is given by

$$x_{\underline{d}} = \frac{x_3}{x_0 x_4} \left(1 + \frac{y_0}{x_1} + \frac{y_4}{x_2} + \frac{y_0 y_1 x_0}{x_1 x_2} + \frac{y_0 y_4}{x_1 x_2} + \frac{y_2 y_4 x_1 x_4}{x_2 x_3} + \frac{y_0 y_1 y_4 x_0}{x_1 x_2^2} \right)$$

$$+ \frac{y_0 y_1 y_2 x_0 x_4}{x_2 x_3} + \frac{y_0 y_2 y_4 x_4}{x_2 x_3} + \frac{2y_0 y_1 y_2 y_4 x_0 x_4}{x_2^2 x_3} + \frac{y_0 y_1 y_2 y_3 y_4 x_0 x_4}{x_2 x_3}$$

$$+ \frac{y_0 y_1 y_2^2 y_4 x_0 x_1 x_4^2}{x_2^2 x_3^2} + \frac{y_0 y_1 y_2^2 y_3 y_4 x_0 x_1 x_4^2}{x_2 x_3^2} \right).$$

The cluster variable's Laurent expansion can be seen term by term using the edge weighting in the poset in Figure 13.

This example is made precise through the following formula mimicking [MSW11].

Theorem 61 (Expansion Formula). Let D be the mixed dimer configuration in P obtained from flipping tiles t_1, \ldots, t_ℓ from M_- . Define the height monomial of D by

$$y(D) = \prod_{i=1}^{\ell} y_i$$

i.e. y(D) is the product of all y_i for which a flip occurred at tiles i to obtain D from M_- . Define $x(D) = \prod_{e \in D} w(e)$ to be the weight of the dimer configuration D. Then the cluster variable associated to (Q,\underline{d}) is given by

$$x_{Q,\underline{d}} = \frac{1}{\underline{x}^{\underline{d}}} \sum_{D \in P} x(D)y(D).$$

Proof. We proceed by induction on k = |d|, the number of allowable flips from M_- in the poset P. When k = 0, our poset has one element, M_- . The associated F-polynomial is 1 and $\underline{x}^{\underline{g}} = w(M_-)$ and our expansion holds. Assume by induction that our claim holds up to $k \in \mathbb{N}$. We aim to show that if k + 1 flips occurred from M_- i.e. $|\underline{d}| = k + 1$ to obtain the maximal mixed dimer configuration D', then our expansion formula holds. It suffices to show that the term in the expansion associated to D' is $\frac{1}{\underline{x}^{\underline{d}}}x(D')y(D')$. By definition of the height monomial $y(\cdot)$, we have that y_i 's account for flipping at each $d_i > 0$ which gives that the y_i 's are indeed $y(D') = \underline{y}^{\underline{d}}$. Moreover, if the $k + 1^{\text{st}}$ flip occurred at tile i, we have the weighting of the x's is changed by dividing by x_j where $j \to i$ in Q and multiplying by x_ℓ when $i \to \ell$ in Q. Hence, the x term in the term corresponding to D' is indeed x(D'). Therefore, we have that

$$x_{Q,\underline{d}} = \frac{1}{\underline{x}^{\underline{d}}} \sum_{D \in P} x(D)y(D).$$

6 Future Directions

In terms of future directions, there are a few possible avenues. For example, we would like to extend our model beyond the acyclic case. If we were to not rely on Tran's model for our proof, which requires that our quiver be acyclic, then we could potentially try to extend our dimer configuration model to apply beyond the acyclic case. Perhaps there is a proof of our model using recurrences of the F-polynomial or representation theory that we could utilize to use this model in less restrictive settings. (Note in Postscript: Between submission and acceptance, together with Libby Farrell, the two authors have succeeded at such an extension [FMW22].)

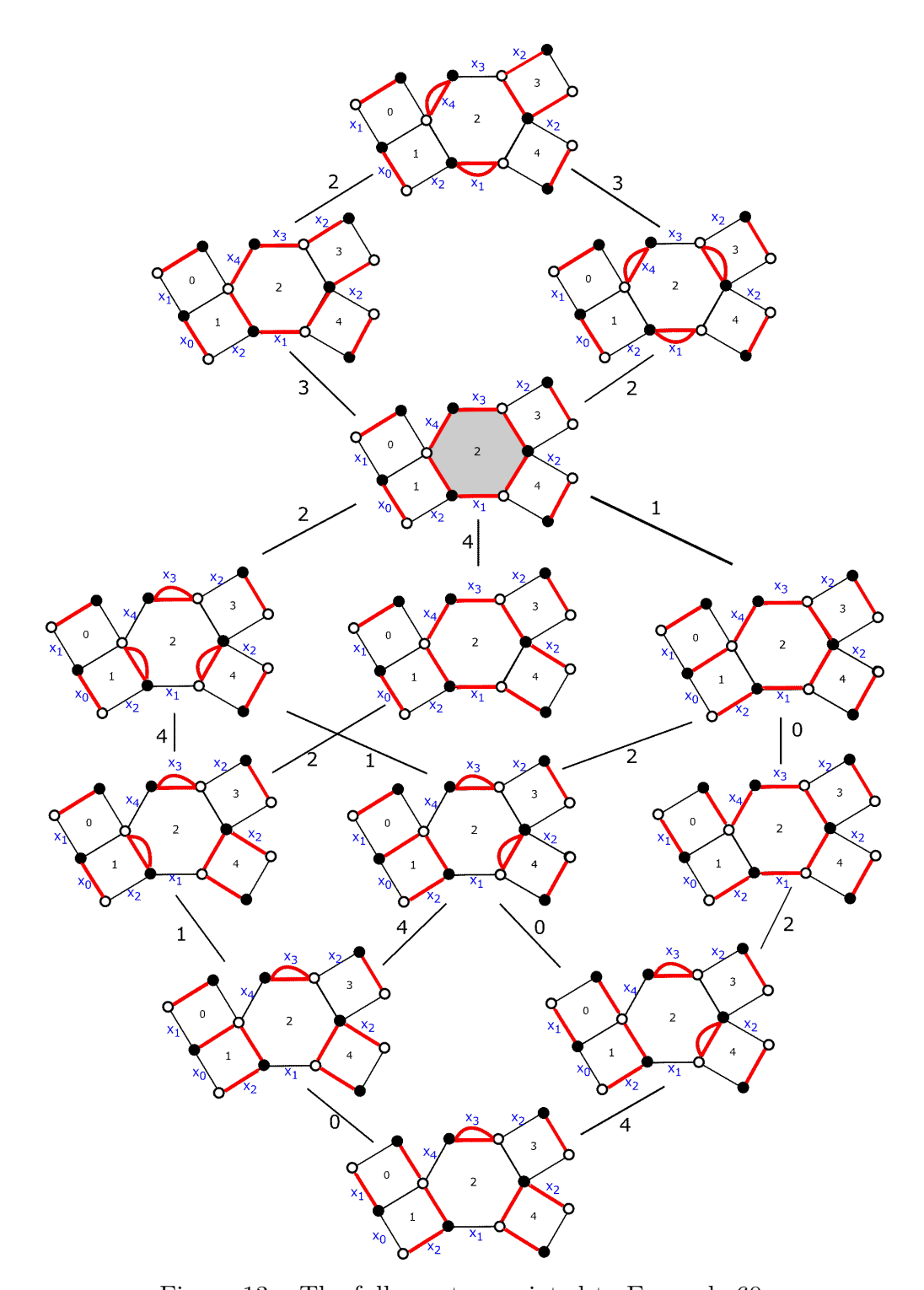


Figure 13 – The full poset associated to Example 60.

Another possible direction would be to try to find a connection between our dimer configuration model and to the punctured disk model with a possible comparison to formulas for tagged arcs from [MSW11]. The punctured disk model is the surface model for type D cluster algebras. When working with surfaces with punctures, i.e. marked points in the interior of the surface, we can use the notion of tagged arcs in a triangulation which can then be translated into γ -symmetric matchings of an associated snake graph. We suspect that there is a way we can use a double dimer configuration model via an "unfolding" method, which is similar to our methods from this paper, to give the connection between double dimer configurations and the surface model. In addition to this question, a paper from 2020 simplifies and unifies the approaches of [MSW11] by considering "good matchings of loop graphs" [Wil20]. These loop graphs add additional structure to the snake graphs in [MSW11] in order to provide a framework to write expansion formulae for the variables corresponding to any tagged arc in a surface. With this new machinery, we wonder if using this additional structure on our dimer configurations could help find the precise connection to the punctured disk model or yield any other interesting generalizations.

We also believe our interpretation is of independent combinatorial interest for the case of type D_n cluster algebras, especially since these arise as cases of the recently investigated cluster structures of Schubert varieties [SSBW19]. This new model for cluster variables has the potential to be extended to other cluster algebras - potentially shedding light on cluster structures on various Grassmannians. Namely, we believe that this mixed dimer configuration approach can improve our understanding of certain cluster variables that arise as quadratic differences in terms of Plücker coordinates. In particular, it is of interest to see if we could embed our base graphs into the disk to create plabic graphs, and relate them to cluster algebras from Schubert varieties. This may dovetail with recent work in progress of Moriah Elkin [Elk21], which has been followed up by joint work in progress with the two authors [EMW22]. We have conjectural double and triple dimer interpretations for Laurent expansions associated to cluster variables in cluster algebras associated to Grassmannians of types Gr(3,6), Gr(3,7), and Gr(3,8).

References

- [BMPW09] Mireille Bousquet-Mélou, James Propp, and Julian West. Perfect matchings for the three-term Gale-Robinson sequences. *Electron. J. Combin.*, 16(1):#P125, 2009.
- [CC06] Philippe Caldero and Frédéric Chapoton. Cluster algebras as Hall algebras of quiver representations. *Commentarii Mathematici Helvetici*, 81(3):595–616, 2006.
- [DF14] Philippe Di Francesco. T-systems, networks and dimers. Comm. Math. Phys., 331(3):1237–1270, 2014.

- [DWZ10] Harm Derksen, Jerzy Weyman, and Andrei Zelevinsky. Quivers with potentials and their representations ii: applications to cluster algebras. *Journal of the American Mathematical Society*, 23(3):749–790, 2010.
- [EF12] Richard Eager and Sebastián Franco. Colored bps pyramid partition functions, quivers and cluster transformations. *Journal of High Energy Physics*, 2012(9):38, 2012.
- [Elk21] Moriah Elkin. Patterns from Gr(3,6), Gr(3,7), and Gr(3,8). UROP Project, Spring 2021.
- [EMW22] Moriah Elkin, Gregg Musiker, and Kayla Wright. Twists of Grassmannian cluster algebras of finite type. In Progress, 2022.
- [FHV⁺06] Sebastián Franco, Amihay Hanany, David Vegh, Brian Wecht, and Kristian D Kennaway. Brane dimers and quiver gauge theories. *Journal of High Energy Physics*, 2006(01):096, 2006.
- [FMW22] Libby Farrell, Gregg Musiker, and Kayla Wright. Mixed dimer configuration model in type d cluster algebras ii: Beyond the acyclic case. arXiv:2211.08569, 2022.
- [FWZ16] S Fomin, L Williams, and A Zelevinsky. Introduction to cluster algebras. chapters 1-3, preprint (2016). arXiv:1608.05735, 2016.
- [FZ02] Sergey Fomin and Andrei Zelevinsky. Cluster algebras i: foundations. *Journal* of the American Mathematical Society, 15(2):497–529, 2002.
- [FZ03a] Sergey Fomin and Andrei Zelevinsky. Cluster algebras ii: Finite type classification. *Inventiones mathematicae*, 154(1):63–121, 2003.
- [FZ03b] Sergey Fomin and Andrei Zelevinsky. Y-systems and generalized associahedra. *Annals of Mathematics*, 158(3):977–1018, 2003.
- [FZ07] Sergey Fomin and Andrei Zelevinsky. Cluster algebras iv: coefficients. *Compositio Mathematica*, 143(1):112–164, 2007.
- [GHKK18] Mark Gross, Paul Hacking, Sean Keel, and Maxim Kontsevich. Canonical bases for cluster algebras. *Journal of the American Mathematical Society*, 31(2):497–608, 2018.
- [GL19] Pavel Galashin and Thomas Lam. Positroid varieties and cluster algebras. arXiv:1906.03501, 2019.
- [Gli11] Max Glick. The pentagram map and Y-patterns. Advances in Mathematics, 227(2):1019–1045, 2011.
- [GW17] Max Glick and Jerzy Weyman. Gale-Robinson quivers: from representations to combinatorial formulas. arXiv:1710.09765, 2017.
- [HV07] Amihay Hanany and David Vegh. Quivers, tilings, branes and rhombi. *Journal of High Energy Physics*, 2007(10):029, 2007.
- [Jen19] Helen Jenne. Combinatorics of the double-dimer model. arXiv:1911.04079, 2019.

- [JMZ13] In-Jee Jeong, Gregg Musiker, and Sicong Zhang. Gale-Robinson sequences and brane tilings. Discrete Mathematics & Theoretical Computer Science, 2013.
- [KP16] Richard W. Kenyon and Robin Pemantle. Double-dimers, the Ising model and the hexahedron recurrence. *Journal of Combinatorial Theory, Series A*, 137:27–63, 2016.
- [KW10] Richard W. Kenyon and David B Wilson. Double-dimer pairings and skew Young diagrams. arXiv:1007.2006, 2010.
- [Lam15] Thomas Lam. Dimers, webs, and positroids. *Journal of the London Mathematical Society*, 92(3):633–656, 2015.
- [LM17] Tri Lai and Gregg Musiker. Beyond Aztec castles: Toric cascades in the dP³ quiver. Communications in Mathematical Physics, 356(3):823–881, 2017.
- [LM20] Tri Lai and Gregg Musiker. Dungeons and dragons: Combinatorics for the dP³ quiver. *Annals of Combinatorics*, pages 1–53, 2020.
- [LMNT14] Megan Leoni, Gregg Musiker, Seth Neel, and Paxton Turner. Aztec castles and the dP³ quiver. *Journal of Physics A: Mathematical and Theoretical*, 47(47):474011, 2014.
- [LS15] Kyungyong Lee and Ralf Schiffler. Positivity for cluster algebras. *Annals of Mathematics*, pages 73–125, 2015.
- [MS10] Gregg Musiker and Ralf Schiffler. Cluster expansion formulas and perfect matchings. *Journal of Algebraic Combinatorics*, 32(2):187–209, 2010.
- [MS16] Robert J Marsh and JS Scott. Twists of Plücker coordinates as dimer partition functions. *Communications in Mathematical Physics*, 341(3):821–884, 2016.
- [MS17] Greg Muller and David E Speyer. The twist for positroid varieties. *Proceedings* of the London Mathematical Society, 115(5):1014–1071, 2017.
- [MSW11] Gregg Musiker, Ralf Schiffler, and Lauren Williams. Positivity for cluster algebras from surfaces. *Advances in Mathematics*, 227(6):2241–2308, 2011.
- [MSW13] Gregg Musiker, Ralf Schiffler, and Lauren Williams. Bases for cluster algebras from surfaces. *Compositio Mathematica*, 149(2):217–263, 2013.
- [Mus07] Gregg Musiker. A graph theoretic expansion formula for cluster algebras of classical type. arXiv:0710.3574, 2007.
- [Pos06] Alexander Postnikov. Total positivity, Grassmannians, and networks. arXiv:math/0609764, 2006.
- [Pro02] James Propp. Lattice structure for orientations of graphs. arXiv:math/0209005, 2002.
- [Pro05] James Propp. The combinatorics of frieze patterns and Markoff numbers. arXiv:math/0511633, 2005.

- [PW18] Piriyakorn Piriyatamwong and Caledonia Wilson. Dimer interpretations in cluster algebras. *Unpublished*, 2018.
- [Sco06] Joshua S Scott. Grassmannians and cluster algebras. *Proceedings of the London Mathematical Society*, 92(2):345–380, 2006.
- [Spe07] David E Speyer. Perfect matchings and the octahedron recurrence. *Journal of Algebraic Combinatorics*, 25(3):309–348, 2007.
- [SSBW19] Khrystna Serhiyenko, Melissa Sherman-Bennett, and Lauren Williams. Cluster structures in Schubert varieties in the Grassmannian. *Proceedings of the London Mathematical Society*, 119(6):1694–1744, 2019.
- [Tra09] Thao Tran. Quantum F-polynomials in classical types. arXiv:0911.4462, 2009.
- [Wil20] Jon Wilson. Surface cluster algebra expansion formulae via loop graphs. arXiv:2006.13218, 2020.
- [YZ08] Shih-Wei Yang and Andrei Zelevinsky. Cluster algebras of finite type via Coxeter elements and principal minors. *Transformation Groups*, 13(3-4):855–895, 2008.